

Photonic time-temperature sensor having an embossed interpenetrating network of cholesteric liquid crystalline polymers and a secondary polymer

Citation for published version (APA):

Kragt, A. J. J., Schenning, A. P. H. J., Broer, D. J., Bastiaansen, C. W. M., Nickmans, K., & Moirangthem, M. (2018). Photonic time-temperature sensor having an embossed interpenetrating network of cholesteric liquid crystalline polymers and a secondary polymer. (Patent No. *WO2018033595*).
https://nl.espacenet.com/publicationDetails/biblio?CC=WO&NR=2018033595A1&KC=A1&FT=D&ND=3&date=20180222&DB=&locale=nl_NL#

Document status and date:

Published: 22/02/2018

Document Version:

Publisher's PDF, also known as Version of Record (includes final page, issue and volume numbers)

Please check the document version of this publication:

- A submitted manuscript is the version of the article upon submission and before peer-review. There can be important differences between the submitted version and the official published version of record. People interested in the research are advised to contact the author for the final version of the publication, or visit the DOI to the publisher's website.
- The final author version and the galley proof are versions of the publication after peer review.
- The final published version features the final layout of the paper including the volume, issue and page numbers.

[Link to publication](#)

General rights

Copyright and moral rights for the publications made accessible in the public portal are retained by the authors and/or other copyright owners and it is a condition of accessing publications that users recognise and abide by the legal requirements associated with these rights.

- Users may download and print one copy of any publication from the public portal for the purpose of private study or research.
- You may not further distribute the material or use it for any profit-making activity or commercial gain
- You may freely distribute the URL identifying the publication in the public portal.

If the publication is distributed under the terms of Article 25fa of the Dutch Copyright Act, indicated by the "Taverne" license above, please follow below link for the End User Agreement:

www.tue.nl/taverne

Take down policy

If you believe that this document breaches copyright please contact us at:

openaccess@tue.nl

providing details and we will investigate your claim.



(51) International Patent Classification:

G01K 3/04 (2006.01) C09K 19/40 (2006.01)
C09K 19/38 (2006.01) C09K 19/04 (2006.01)

(21) International Application Number:

PCT/EP2017/070837

(22) International Filing Date:

17 August 2017 (17.08.2017)

(25) Filing Language:

English

(26) Publication Language:

English

(30) Priority Data:

16184490.7 17 August 2016 (17.08.2016) EP
62/462,180 22 February 2017 (22.02.2017) US

(71) Applicant: TECHNISCHE UNIVERSITEIT EINDHOVEN [NL/NL]; Den Dolech 2, 5612 AZ Eindhoven (NL).

(72) Inventors: KRAGT, Augustinus Jozef Johannes; Multatuliplaats 22A, 6531 DW Nijmegen (NL). SCHENNING, Albertus Petrus Henricus Johannes; Vogelwikke 51,

5531 KA Bladel (NL). BROER, Dirk Jan; Bovenland 7, 5663 HP Geldrop (NL). BASTIAANSEN, Cornelis Wilhelmus Maria; Burg. Geurtsweg 3, 6065 EE Montfort (NL). NICKMANS, Koen; Ds. Theodor Fliednerstraat 189, 5631 MD Eindhoven (NL). MOIRANGTHEM, Monali; Hemelrijken 223, 5612 WP Eindhoven (NL).

(74) Agent: DELTAPATENTS B.V.; Fellenoord 370, 5611 ZL Eindhoven (NL).

(81) Designated States (unless otherwise indicated, for every kind of national protection available): AE, AG, AL, AM, AO, AT, AU, AZ, BA, BB, BG, BH, BN, BR, BW, BY, BZ, CA, CH, CL, CN, CO, CR, CU, CZ, DE, DJ, DK, DM, DO, DZ, EC, EE, EG, ES, FI, GB, GD, GE, GH, GM, GT, HN, HR, HU, ID, IL, IN, IR, IS, JO, JP, KE, KG, KH, KN, KP, KR, KW, KZ, LA, LC, LK, LR, LS, LU, LY, MA, MD, ME, MG, MK, MN, MW, MX, MY, MZ, NA, NG, NI, NO, NZ, OM, PA, PE, PG, PH, PL, PT, QA, RO, RS, RU, RW, SA, SC, SD, SE, SG, SK, SL, SM, ST, SV, SY, TH, TJ, TM, TN, TR, TT, TZ, UA, UG, US, UZ, VC, VN, ZA, ZM, ZW.

(54) Title: PHOTONIC TIME-TEMPERATURE SENSOR HAVING AN EMBOSSED INTERPENETRATING NETWORK OF CHOLESTERIC LIQUID CRYSTALLINE POLYMERS AND A SECONDARY POLYMER

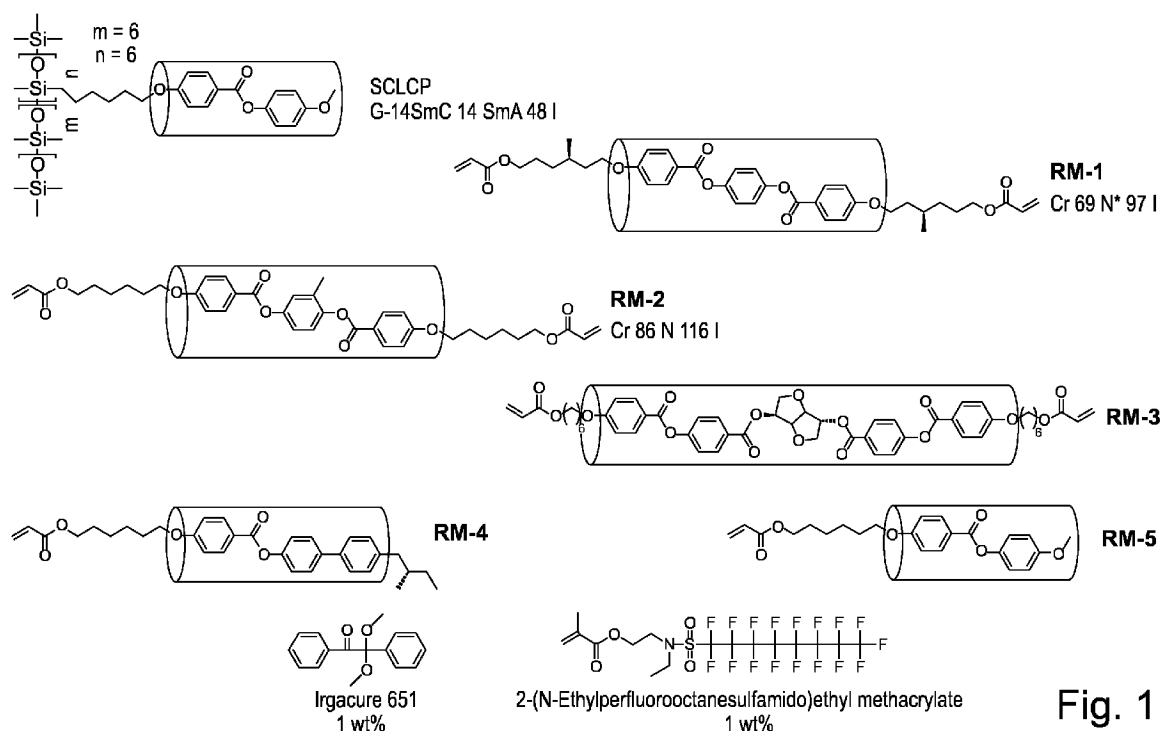


Fig. 1

(57) Abstract: Photonic time-temperature sensor consisting of an embossed interpenetrating network of a cholesteric liquid crystalline polymers and a secondary polymer. Preferably in which the secondary polymer is orthogonal and is not covalently attached to the interpenetrating network, but physically interpenetrated therein. For use as food sensor for checking freshness of the food.

(84) Designated States (*unless otherwise indicated, for every kind of regional protection available*): ARIPO (BW, GH, GM, KE, LR, LS, MW, MZ, NA, RW, SD, SL, ST, SZ, TZ, UG, ZM, ZW), Eurasian (AM, AZ, BY, KG, KZ, RU, TJ, TM), European (AL, AT, BE, BG, CH, CY, CZ, DE, DK, EE, ES, FI, FR, GB, GR, HR, HU, IE, IS, IT, LT, LU, LV, MC, MK, MT, NL, NO, PL, PT, RO, RS, SE, SI, SK, SM, TR), OAPI (BF, BJ, CF, CG, CI, CM, GA, GN, GQ, GW, KM, ML, MR, NE, SN, TD, TG).

Declarations under Rule 4.17:

— *as to applicant's entitlement to apply for and be granted a patent (Rule 4.17(ii))*

Published:

— *with international search report (Art. 21(3))*

PHOTONIC TIME-TEMPERATURE SENSOR HAVING AN EMBOSSED INTERPENETRATING NETWORK OF CHOLESTERIC LIQUID CRYSTALLINE POLYMERS AND A SECONDARY POLYMER.

5 **BACKGROUND**

A time-temperature sensor is a device or smart label that shows the accumulated time-temperature history of a product. Time temperature sensors are commonly used in food, pharmaceutical and medical products to indicate previous exposure to (excessive) temperature. In some cases, such sensors or indicators can also provide an indication of how much time was spent at an (excessive) temperature. In particular for use as indicators of food freshness such sensors become increasingly important. At the Eindhoven University of Technology in the Netherlands so-called “fresh strips” are being developed. These strips refer to a technology that changes colour of the strips to indicate whether foods or medical supplies have been exposed to excessively high temperatures and can still be consumed or used. In US 20130148690 A1 a time-temperature indicator (TTI) is described which uses ‘polymer hardening properties to “set” or retain indications of the temperature history. The TTI includes a mesh layer affixed to a thermo-conductive adhesive layer and a photonic crystal patterned film affixed to the mesh layer. The TTIs are put in or on the food products or are integrated into their packaging, and in case of temperature abuse or when the product reaches its “use-by” date, the temperature-dependent growth of the TTI microorganisms causes a pH drop in the tags, thereby leading to an irreversible color change of the medium chromatic indicator which becomes red.

25

DEFINITIONS

For the purpose of this patent application, unless separately defined hereinbefore or elsewhere in this patent application, terms, including abbreviations used herein, have the meaning as defined hereunder.

30

‘embossing’ is the process of creating either raised or recessed relief images or designs in paper, synthetic or natural polymers and other materials.

‘embossed film’ refers to a film in which either raised or recessed relief images or designs have been created.

35

‘sensor’ and ‘indicator’ have the same meaning, i.e. indicating change.

‘TTI’ refers to both time temperature indicator and time temperature integrator.

'RM' refers to reactive mesogen, i.e. polymerisable mesogen.

'chiral' refers to non-superimposable on its mirror image.

'LCP' refers to liquid crystalline polymers.

'SCLCP' refers to side chain liquid crystalline polysiloxane.

5 'CLC' or 'ChLC' refers to cholesteric liquid crystal.

'LMWLC' refers to low molecular weight (non-reactive) liquid crystal.

'cholesteric liquid crystal' refers to a liquid crystal with a helical structure and which is therefore chiral.

'SMP' refers to shape memory polymer.

10 'IPN' refers to interpenetrating polymer network.

'POM' refers to Polarized Optical Microscopy.

'elastomer' refers to a polymer with elastomeric behaviour i.e.entropy driven reversible stress-strain behaviour.

15 'nematic phase' refers to nematic liquid crystal phase characterized by molecules that have no positional order but tend to point in the same direction (along the director).

'isotropic phase' refers to disorder of molecules in all directions.

20 'switchable polymer' refers to a stimulus-sensitive polymer having shape memory or which is capable of undergoing transformation from one phase to another phase under influence of a stimulus, e.g. a change in temperature. Such may induce a transition from a cholesteric phase to an isotropic phase at a certain temperature.

25 'cholesteric phase' refers to the nematic state superimposed with a twist including the long axis of the molecules induced by the incorporation of a chiral group to give a helical twist to the orientation of the director.

'suitable' refers to what a person skilled in the art would consider technically required for the purpose, which is without undue burden technically feasible and for which no inventive effort or undue experimentation is required to arrive at.

'optics' refers to the behaviour of visible, ultraviolet, and infrared light.

30 'photonic' refers to the practical application of optics.

'photonic time-temperature indicator' refers to an irreversible time-temperature photonic sensor.

'The inventors concerned' refers to a group of inventors, mutatis mutandis, working or having been working together.

'food sensor' refers to a photonic time-temperature indicator or other photonic indicators indicating other mitigating factors for food safety such as pH, humidity, CO₂, O₂, etc.

5 'orthogonal polymer' refers to a polymer which has disparate physical or mechanical properties to the cholesteric liquid crystal polymer network and which does not interfere with the properties of the latter.

For the definition of other terms, not defined above or hereinafter, reference is made to published patent specifications and/or published scientific papers including theses, in
10 which such terms have already been defined. These can without undue effort be found on the internet.

PROBLEM

15 Photonic sensors have been reported in the prior art which consist of an embossed cholesteric liquid crystalline polymer film. These sensors work based on a shape memory effect which is induced by heat. Around a specific transition temperature (which often coincides with the glass transition temperature of the material), the embossed film relaxes back to the pre-embossed state, inducing a colour
20 change in the material. Understandably, the material properties of the cholesteric polymer film are key to its thermomechanical response. However, the limited control in temperature range and sensitivity and the cross-sensitivity has thus far limited the applicability in sensors:

- 25 1. The glassy (brittle) nature of the films limits their ability to be embossed in the first place, which limits the shape change and therefore colour response.
2. The transition temperature is typically too high for most refrigerated substances (above 30°C).
3. The transition is relatively sharp, which limits the "temperature integration" effect.
30 4. Tuning the transition temperature, as required for a specific application, is relatively difficult.

So far one has tried to solve the problem, but current solutions are too expensive for commercial application. A variety of electronic sensors is on the market
35 which can serve as time-temperature integrators. These electronic sensors typically cost more than 1 Euro/sensor and are far too expensive for the intended applications (price

should be less than 0.05 Euro/sensor. Further other time-temperature integrators are on the market but they generally consist of multiple layer devices, making them more expensive. Also, special devices such as electronic or optical noses are often required for the read-out of the sensors which further limits practical applications

5

SOLUTION

For different applications of these sensors one needs to be able to change the transition temperature easily and at will, without disturbing the properties of the cholesteric network (the liquid crystalline behaviour). The invention describes a solution in the form of an interpenetrating network (IPN) consisting of a cholesteric liquid crystalline polymer network and a second orthogonal polymer. The polymer is not covalently attached to the cholesteric network, but physically interpenetrated. Said polymer may or may not be liquid crystalline in nature. By changing the material properties of this polymer (chemistry) or amount added (volume fraction), the material properties of the IPN can be easily tuned.

The key to the invention is the combination of the two materials described above into an IPN and its subsequent processing into an irreversible time-temperature photonic sensor by for example mechanical embossing. The inventiveness lies in the combination of such IPNs with its processing (printing, curing, mechanical embossing), in order to obtain photonic sensors that show a large colour response (sensitivity) which is also easily tuneable. The inventors (see previously) concerned believe that in this way the last technological hurdle has been overcome in order to commercialize these materials as affordable photonic sensors. These and other aspects of the invention will be apparent from and elucidated further with reference to the embodiments described by way of examples in the following description and with reference to the accompanying figures.

Further, as mentioned hereinbefore other time-temperature integrators are on the market but they generally consist of multiple layer devices, making them more expensive. The present invention relates to a photonic time-temperature indicator that is consisting of an embossed interpenetrating network of cholesteric liquid crystalline polymers and a secondary polymer.

35

The present invention further relates to a process for preparing a formulation consisting of reactive liquid crystal mesogens and a compatible secondary polymer.

The process comprises the following steps:

- 5 1. Preparing a formulation consisting of reactive liquid crystal mesogens and a compatible secondary polymer. This polymer has a suitably low glass transition temperature, for example but not limited to a poly(dimethylsiloxane) or derivatives thereof.
- 10 2. Printing a thin layer (3-20 μm) of said formulation onto a substrate with a (rubbed) alignment layer by conventional LC processing techniques (screen, flexographic, inkjet printing, bar-coating, slit die coating etc).
3. Polymerizing the layer, for instance, by UV-irradiation to form the interpenetrating network.
- 15 4. Mechanical embossing of the layer at an appropriate temperature and load, higher than the glass transition temperature (-20 to 60°C) to induce the photonic memory effect.
5. Cooling the layer to the application temperature range below the glass transition temperature, to "lock-in" the photonic memory effect.

20

PRIOR ART AND ADVANCEMENT OF THE ART BY THE PRESENT INVENTION

WO2010084010 (A1), published 22 January 2009 describes an invention related to multifunctional optical sensor, having at least two areas which independently react to different input parameters, the sensor comprising a substrate and a polymeric
25 layer comprising polymerized liquid crystal monomers having an ordered morphology, wherein the color, the reflectivity or the birefringence of the sensor changes due to a change of the morphology, wherein said change of the morphology is caused by physical contact with a chemical agent such as a gas or liquid a change of temperature, or passage of time. The invention also relates to a process for the
30 preparation of the sensor and for the use of a film comprising a single substrate, a layer having a cholesteric liquid crystalline structure for application in labels for packaging of perishable goods, food, fine chemicals, bio-medical materials.

EP 2623927 A1, published 7 August 2013 with filing date 2 February 2012, also
35 published as WO 2013113877 A1, published 8 August 2013 with filing date 1 February 2013, describes an invention related to the use of an arrangement of a substrate and a

liquid crystal layer provided on the substrate as an optical strain sensor, wherein the liquid crystal layer comprises liquid crystalline molecules having an ordered morphology and wherein the optical properties of the liquid crystal layer change by the strain of the substrate.

5

According to the inventors concerned, as to the present invention, the combination of materials into an IPN in combination with mechanical embossing for sensors is new.

The present invention relates specifically to a photonic sensor which act as time-temperature integrator. Such sensors have, for instance, a variety of applications in food and medical products

In the past, sensors in food applications have been minimal primarily due to the high cost of implementation and given the traditionally low operating margins (around 1%) under which the food industry operates both in production and in retail.

15

The advancement of the art by the present invention lies in the possibility of providing a novel low-cost time-temperature integrator which consists of a single layer of plastic which can be easily printed on packaging containers of e.g. food, drugs and the like at relatively low cost.

20

It has been discovered that the present invention makes it possible to change the broadness of the thermal transition, without disturbing the properties of the cholesteric network. This is necessary in order to tune the temperature response of the sensor (fast vs. slow response).

25

According to the inventors concerned commercially available TTIs cost more than \$1 per piece:

<http://www.omega.com/pptst/TSDC-9000-16.html#order> <https://www.amazon.com/3M-MonitorMark-TemperatureIndicator9860B/dp/B00JFRJ1Q8>

30

Smaller companies are also developing TTIs based on alternative technologies. For example, thermochromic inks may also be cost-effective but no pricing is available.

<http://www.insigniatechnologies.com/technology.php>

The cost of the indicators according to the present invention is minimal because very little material is required to make the sensor. Furthermore the sensors can be produced

using roll to roll techniques in combination with high speed printing techniques. For example, to produce a sensor of dimensions 1 cm * 1 cm * 10 micron, would cost 0.24 eurocent in material costs. (assumption monomers price = 2000 euro/kg.).

- 5 State of the art multilayer devices generally make use of more material (materials cost) take multiple processing steps for their fabrication due to their added complexity (processing cost). This makes the fabrication of such multilayer devices more expensive.
- 10 According to the inventors concerned the only shape memory cholesteric liquid crystal polymer reported so far, by Davies et. al., showed a minimal optical response to heat (30 nm). Besides that, the optical response was observed in a narrow temperature window of 40°C – 55°C, too high for applications in food and pharma packaging. (D. J. D. Davies, A. R. Vaccaro, S. M. Morris, N. Herzer, A. P. H. J. Schenning, C.W.M. Bastiaansen, Adv. Funct. Mater. 2013, 23, 2723.)
- 15

A broader temperature window from 35°C to 55°C was obtained by DiOrio et. al. with spatially graded glass transition temperatures from a thiol-ene based photo-crosslinkable glassy thermoset, but the system lacked optical response. (A. M. DiOrio, X. Luo, K. M. Lee, P. T. Mather, Soft Matter 2010, 7, 68.)

20

CLAIMS

The description hereinafter of the claims specifying the exclusive rights on the present invention is deemed to be included in the description of this patent application. These exclusive rights cover also embodiments of the present invention not covered by the explicit wording of the claims but nevertheless forming obvious embodiments of the present invention for a person skilled in the art.

25

30

BRIEF DESCRIPTION OF THE FIGURES

Figure 1: Pool of molecules used for the fabrication of cholesteric coatings.

Figure 2 A Transmission spectra of coatings prepared from (A) M1, M2 and M3 and (B) M4 and M5 at 30 °C and 120 °C. At 500 nm the sequence of the graphs from bottom to top is; M1 30 °C, M1 120 °C, M3 30 °C, M2 30 °C, M2 120 °C, M3 120 °C.

35

Figure 2 B: At 500 nm the sequence of the graphs from bottom to top is; M4 30 °C, M5 30 °C, M4 120 °C, M5 120 °C.

Figure 3: Reversible blue- and red shifting with temperature.. At 500 nm the sequence of the graphs from bottom to top is; 25 °C end, 80 °C t = 39 min, 21 °C initial, 80 °C t = 0 min.

Figure 4: Molecular structure of the components used for fabrication of the semi-interpenetrating network of cholesteric polymer and poly(benzyl acrylate).

Figure 5: (a) UV-Vis spectrum of semi-interpenetrating network (semi-IPN) of cholesteric polymer and poly(benzyl acrylate). Inset shows the image of the semi-IPN film. (b) DSC curve of the semi-IPN film. Rate of heating and cooling was maintained at 20 °C min⁻¹.

Figure 6: (a) TEM cross-section image of the semi-interpenetrating network (semi-IPN) (highlighted in green) of the cholesteric polymer and poly(benzyl acrylate), embedded in epoxy resin. (b) and (e) show the top and bottom, and (c) and (d) show the middle part of the cross-section of the semi-IPN film. The spacing between the two bright (or two dark) bands that represents half a pitch increases in the middle of the film.

Figure 7: (a) Schematic representation of the steps followed in the mechanical embossing experiment of the photonic polymer film. (b) Images of the polymer film captured on increasing temperature shows change in color from blue to orange. The images of the film at temperatures 8 °C and above were captured after 7 hrs (c) UV-vis transmission spectra of the embossed area of the photonic polymer film shows red shift of the reflection band on increasing temperature from 0 °C to 75 °C. The film was kept at each temperature for 1 hour (d) Height profile of the embossed area at room temperature shows a spherical indentation as deep as ~ 6 μm at the lowest point. At 475 nm the sequence of the graphs from bottom to top is: 0 °C, 20 °C, 35 °C, 75 °C.. The graph of 55 °C is hidden.

Figure 8: Optical response, $\Delta\lambda$, of the embossed area of the photonic film at a temperature T after 1 hr for two different heating routes.

Figure 9: (a) Observed red shifts of the reflection band ($\Delta\lambda$) of the central embossed area of different photonic films after 7 hr at various temperatures. The red curve is the fitted curve of the data points. (b) Observed red shifts of the reflection band ($\Delta\lambda$) of the central embossed area of a photonic film after 1 hr at low temperatures.

Figure 10: (a) Red shifts ($\Delta\lambda$) of the reflection band of the central embossed area is measured at different temperatures over time with reference to the red shift observed at 75 °C ($\Delta\lambda_{max}$) on complete recovery. (b) Shape recovery data of (a) shown on a

logarithmic time axis. (c) Mastercurve constructed from the data of subgraph (b) using Time-Temperature-Superposition (TTS); solid line is a fit according to Equation 1. (d) Shift factors used to construct the mastercurve; solid line is an Arrhenius fit. The graphs in Figure 10 (a) and Figure 10 (b) from bottom to top correspond with the values indicated in the list next to Figure 10 (b) from 55 C to 8 C upwards. The graph points of the graph in Figure 10 (c) and Figure 10 (d) correspond with the values indicated in the list next to Figure 10 (b) from 55 C to 8 C upwards.

Figure 11: DSC curves for (a) pure cholesteric polymer CLC-5CB and (b) pure homopolymer poly(benzylacrylate). Rate of heating and cooling was maintained at 20 °C min⁻¹.

Figure 12: (a) Image and (b) UV-Vis spectrum of the pristine CLC polymer film and the film after removal of 5CB (CLC-5CB).

Figure 13: Height profile measurement of pristine CLC polymer film, film after removal of 5CB (CLC-5CB), and semi-interpenetrating network (semi-IPN) of the cholesteric polymer and poly(benzyl acrylate). At 1000 μm the sequence of the graphs from bottom to top is: CLC-5CB, Pristine CLC, Semi-IPN.

Figure 14: (a) TEM cross-section image of the pure cholesteric polymer film (CLC-5CB) (highlighted in green) embedded in epoxy resin. (b) and (c) show the top and bottom, and (d) and (e) show the middle part of the cross-section of the cholesteric film. The alternating bright and dark bands are due to the anisotropy arising from the cholesteric orientation. The distance $d = 132$ nm between two bright (or two dark) bands represents half a pitch.

Figure 15: FT-IR curve of the pristine CLC polymer film, film after removal of 5CB (CLC-5CB), and semi-interpenetrating network (semi-IPN) of the cholesteric polymer and poly(benzyl acrylate).

Figure 16: Thermogravimetric analysis of cholesteric polymer film after removal of the porogen 5CB (CLC-5CB) and semi-IPN formed by incorporation of poly(benzyl acrylate). At 500 °C the sequence of the graphs from bottom to top is: CLC-5CB, Semi-IPN.

Figure 17: Amount of red shift of the reflection band ($\Delta\lambda$) of the one step-embossed semi-IPN film observed at various temperature after 1 hour. The red curve is the fitted curve of the data points. The mechanical embossing was done at 75 °C with a load of 5.2 Kg.

Figure 18: UV-Vis transmission spectra of mechanically embossed and non-embossed CLC-5CB (with 4 wt. % chiral dopant LC756 but equal amount of crosslinker) polymer film showed a small difference of 7 nm. The embossing was done at 75 °C with a load

of 5.2 Kg. At 525 λ (nm) the sequence of the graphs from bottom to top is: Embossed, Not embossed.

Figure 19: IPN formed from SCLCP combined with reactive mesogens is coated into film and subsequently polymerized.

5 Figure 20: Siloxane liquid crystal polymer + reactive mesogens composition. With reference to Appendix A, the molecular structures from bottom to top refer to SCLCP, RM-4, RM-1.

Figure 21 B is the same as Figure 3. Referring to reversible blue- and red shifting with temperature.

10

Figure 22: Thermal transitions of the monomer mixtures as determined by DSC. The cholesteric phase is situated between the lines.

Figure 23: Glass transition temperatures of the IPNs. The circle represents the middle of the glass transition. The lines represent the width of the glass transition.

15 Figure 24: Optical micrographs of a 10 micron film after embossing (left), and after heating to 50 °C for 10 minutes (right).

GUIDANCE OF THE SKILLED PERSON

20 In order to successfully carry out the present invention the following is provided as guidance. Alternative solutions which can be selected without an undue burden for the person skilled in the art, are covered by the present invention.

25 EXAMPLES

The present invention is further described and elucidated by the below Appendices A to E inclusive.

30 *Appendix A – Temperature responsive coatings based on reactive mesogens and liquid crystal polymers*

Introduction.

35 Stimulus-responsive reflective systems based on cholesteric liquid crystals are a growing research area for applications, such as decorative paints, sensors and smart windows. Usually these systems are based on mixtures of reactive mesogens (RMs) and low molecular weight liquid crystals (LMWLCs) of which the optical and responsive

properties can be tuned in a modular approach. However, these mixtures are limited to encapsulated or closed cell systems, due to the volatility of LMWLCs and thus less suitable for coating application. The main goal of this project is to prepare easy coatable, tunable and temperature-responsive reflective coatings. Our approach so far is to use thermally stable flexible liquid crystalline polymers (LCP) in combination with reactive mesogens.

Cholesteric coatings based on mixtures of RMs and LCPs.

Various RMs (chiral and achiral) were mixed with an achiral side chain liquid crystal polymer (SCLCP) together with a photo initiator and surfactant (both 1 wt%) (fig. 1). It was shown that the reflective wavelength of these cholesteric mixtures could be tuned by the concentration of chiral RM. We also found that these mixtures could easily be processed to a film using knife coating. In addition these films could be patterned using photomask polymerization. These properties emphasizes some important advantage of using RMs.

Temperature dependent reflection band intensity.

Coatings in which the reactive mesogens were only diacrylates showed a reversible decrease in reflection band intensity (fig. 2). The level of decrease was found to be strongly dependent on the concentration of diacrylate, which limited the temperature response for mixtures **M1** and **M2** (25.5 and 21 wt% diacrylate respectively) (fig. 2A). To increase the temperature-response for coatings in the visible region a chiral diacrylate with a high helical twisting power (**RM-3**) was used to fabricate coatings reflecting in the visible region with only 15 wt% diacrylate (**M4** and **M5**) (fig. 2B).

Temperature dependent reflection band shifting.

By reducing the crosslink density of the network by replacing some diacrylates to monoacrylates the network was able to contract when the SCLCP side chains loses their order and a blue shift occurred. By storing the coatings overnight at a temperature just below the clearing temperature (45 °C) the SCLCP side chains were able to organize themselves again to the original state partly and thus the reflection band red shifted to some extent. From this point onwards the coatings could be reversible blue- and red shifted with temperature (fig. 3). By varying the concentration of diacrylate and monoacrylate the wavelength range between which the reflection band shift takes place could be influenced. A higher concentration of diacrylates led to a smaller blue shift, but increased the red shifting capabilities of the coatings till a certain plateau. The

influence of the monoacrylate concentration showed a similar trend, although the influence is weaker. This way coatings could be prepared with a desired colour change, which is interesting for optical sensor applications.

However, for smart window applications the coatings need to be infrared (IR) reflective. When we tuned the initial reflection band in the IR, comparable blue shifts could be observed, but the red shifts were significantly less. The reason for this could be that the spacing between the molecules is larger for larger pitches, meaning that the anchoring forces for the SCLCP side chains needed to organize them again after heating are reduced. In the near future we anticipate on solving this issue by using a dichroic photo initiator to create an accumulation of reactive mesogens every half pitch length. Our aim is that this will provide anchoring forces for all the SCLCP side chains, so that the system becomes fully reversible.

Another way to obtain reversible blue- and red shifting might be the use of a chiral LCP in combination with reactive mesogens. At the moment, this work is executed by a student from the South China Normal University (Weixin Zhang). The first results look promising. For either way, once a fully reversible temperature-responsive blue- and red shifting IR reflector is obtained, work will be done towards a final device. This will include the creation of broadband and 100% IR reflectors. Preliminary studies towards this were done during an OGO project, where multiple layers were coated on top of each other. Also these results were promising.

Appendix B – A Photonic Shape Memory Interpenetrating Polymer Network with a Broad Temperature and Color Response

25 Abstract.

A photonic shape memory polymer film which undergoes a broad thermal transition and shows large color response (~ 155 nm) in a wide range of temperature from 0 to 55 °C has been fabricated from a semi-interpenetrating network of a cholesteric polymer and poly(benzyl acrylate). The large color response was achieved by mechanical embossing of the photonic film above its glass transition temperature. The embossed film, as it recovers to its original shape, exhibits multiple quasi-stable shapes that display distinct colors, clearly visible to the naked eye, as a function of time and temperature; with the effect of temperature much stronger. Such photonic materials are attractive for development of optical temperature sensors, and time-temperature integrators for applications as smart packaging labels.

Introduction.

Shape memory polymers (SMPs) are an interesting class of smart materials as they can be deformed and locked into a temporary shape which, only under the influence of a specific stimulus like heat, solvent, pressure, light etc., recovers back to its original shape.¹⁻⁵ Conventional shape memory polymers have just one temporary shape, termed as dual-shape polymers, which limited their ultimate potentials. However in the past decade, with active investigation on SMPs with more than one temporary shapes, termed as multi-shape polymers, a plethora of potential advanced applications in areas of biomedical devices, drug delivery, morphing aircrafts and reconfigurable smart consumer products have opened up.⁶⁻⁹

Photonic materials¹⁰ which show shape memory effect are of special interest for development of stimuli-responsive optical sensors¹¹⁻¹³, and reconfigurable nanooptical devices.^{14,15} However, shape memory photonic materials are, so far, limited to only dual shape. For instance, macroporous photonic crystals have been shown to exhibit disorder (translucent)-order (iridescent) transition with organic vapors¹³ or pressure^{12,15} as the stimulus. As for the cholesteric liquid crystalline (CLC) based photonic SMPs, they are largely unexplored. The only shape memory CLC polymer, developed by Davies et. al. was responsive to heat and the optical response associated with the transformation of shape was minimal (only 30 nm).¹¹ Besides that, optical response was observed in a narrow temperature window of 40 to 55 °C –high for real application as time-temperature integrators in food and pharmaceutical packaging industries. A broader temperature window from 35 to 55 °C was obtained by DiOrio et. al. with spatially graded glass transition temperatures from a thiol-ene based photo-crosslinkable glassy thermoset.⁶ Due to position-dependent T_g s, different parts of the polymer recover at different temperatures. However, it lacked optical response. Therefore, the challenge is to design a photonic SMP which displays multiple shapes and large optical response in a broad temperature window.

Multi-shape polymers can be produced by incorporating two or more discrete thermal transitions, which could be glass transition (T_g), melting (T_m) or clearing (T_{cl} , in case of liquid crystalline domains) temperatures, into the polymer; the number of temporary shapes is usually equal to the number of transitions. However, the design and fabrication of polymers with more than two strongly bonded and distinct reversible phases is extremely challenging.¹⁶ A more versatile approach is to introduce a broad thermal transition which can be considered as infinite discrete transitions T_{trans} which are so closely spaced that they form a continuum.¹⁶ A polymer with broad thermal transition can, therefore, be tailor-programmed in umpteen ways as per

demand by choosing desired temperatures (one or more) out of the infinite transition temperatures for step-wise deformation and thus, a greater degree of freedom in designing multiple temporary shapes can be achieved.¹⁷

A well-known strategy to produce broad glass transition is to use an interpenetrating polymer network (IPN).¹⁸ Additionally, an IPN also provides the unique opportunity to combine the properties of two different polymers.¹⁹ With CLC polymer²⁰⁻²² as one of the polymers, it renders the IPN with the ability to reflect light due to its one-dimensional photonic structure, and thereby imparting the material the desired dual functionality of optical response as well as broad thermal transition. Such IPN based photonic shape memory materials are appealing for development of easy-to-use time-temperature integrators with optical read-out visible to the naked eye.

Here, we report for the first time on a photonic semi-interpenetrating network (semi-IPN) comprising of a CLC polymer and poly(benzyl acrylate). The photonic film exhibits a broad glass transition (T_g) from 10 to 54 and can be deformed mechanically to a temporary shape, accompanied by a large change in color from orange to blue ($\Delta\lambda \approx 155$ nm). Shape recovery takes place in response to rise in temperature through the T_g by forming multiple intermediate quasi-stable shapes.

Results and discussion

Fabrication and characterization of photonic polymer film.

In order to obtain a photonic polymer film with a broad T_g , a semi-interpenetrating network (semi-IPN) was fabricated from a cholesteric polymer film with a T_g of 60 °C (Figure 11a) and poly(benzyl acrylate) (abbreviated as poly(BA)) whose pure homopolymer has a T_g of ~6 °C (Figure 11b).^{23,24} The benzyl acrylate (BA) monomer can readily penetrate into the cholesteric polymer due to the presence of π - π interaction between the benzene rings of the monomer and the cholesteric polymer, making BA an ideal complementary monomer to make the semi-IPN.²⁵ The semi-IPN film with broad glass transition, on mechanical embossing above its T_g followed by fixing the temporary deformed shape below its T_g , is expected to exhibit multiple intermediate shapes as it recovers on increasing the temperature through the broad T_g .⁶

The cholesteric polymer to make the semi-IPN was fabricated from a monomer mixture including a diacrylate (RM257, 29 wt. %) and a monoacrylate (RM105, 35 wt. %) mesogens (Figure 4). It also contained a non-polymerizable mesogen (5CB, 30 wt. %) to act as a porogen in order to facilitate incorporation of BA monomer.¹⁹ A chiral molecule (LC756, 5 wt. %) with polymerizable end groups was

used to induce cholesteric (or chiral nematic) liquid crystalline phase. Irgacure 651 was added to initiate the photopolymerization reaction. The cholesteric mixture was filled in a polyimide coated cells with 70 μm spacer and was photopolymerized at room temperature to obtain a free-standing green reflecting polymer film (70 μm thick) with selective reflection band (SRB) centered at $\lambda = 515 \text{ nm}$ (Figures 12, 13).

In order to create free volume within the polymer network to accommodate the BA monomers, 5CB was removed by extracting with an organic solvent (tetrahydrofuran). This resulted to a large blue shift of the reflection band to $\lambda = 380 \text{ nm}$ implying shortening of helical pitch length by 26.2 % (Figure 12), which is in good agreement with the 30 % decrease observed in the thickness of the film (Figure 13). TEM images of the cross-section of the film revealed an equally spaced alternating bright and dark bands due to the cholesteric orientation of the molecules (Figure 14).¹⁹ FT-IR curve witnesses disappearance of the peak at 2225 cm^{-1} originating from stretching vibration of ($-\text{C}\equiv\text{N}$) of 5CB (Figure 15). Moreover, no weight loss was observed below 200 $^{\circ}\text{C}$ in the thermogravimetric curve (Figure 16) suggesting complete removal of 5CB.¹⁹ DSC experiments showed that the polymer film undergoes glass transition at 60 $^{\circ}\text{C}$ (Figure 11).

The blue cholesteric polymer film without 5CB (CLC-5CB) was then treated with benzyl acrylate (BA) monomer mixed with 1 wt. % of photoinitiator (Irgacure 651) and this resulted to a change in color from blue to orange due to increase in pitch length caused by the penetration of BA monomers into the cholesteric network. Photopolymerization of the swollen orange film led to formation of the photonic semi-IPN of the cholesteric polymer and poly(BA). A new band centered at 748 cm^{-1} due to the rocking motion of the long ($-\text{CH}_2$) polymer backbone in poly(BA) appeared in the FT-IR spectrum of the semi-IPN (Figure 14). The amount of poly(BA) incorporated was determined by weighing the polymer film before, and after treatment followed by polymerization of BA, and was found to be 42.4 wt. %. Reflection band of the semi-IPN ($\sim 76 \mu\text{m}$ thick, Figure 13) was found to be centered at $\lambda = 590 \text{ nm}$ which translates to 40.8 % increase in pitch length (Figure 5a) – in good agreement with the observed 43 % increase in film thickness. TEM cross-section images of the semi-IPN showed a varying pitch length throughout the thickness of the film –shorter near the top and bottom, and longer in the middle (Figure 6), implying that BA monomers are partially removed from the polymer film while wiping out excess monomers before polymerization. The difference in pitch length manifested as a shoulder around $\lambda = 630 \text{ nm}$ in the reflection band of the semi-IPN (Figure 5a).

The DSC curve of the semi-IPN is markedly different from that of the pure cholesteric polymer CLC-5CB and the pure homopolymer poly(BA). A broad glass transition that onsets at 10 °C (T_{low}) and ends at 54 °C (T_{high}) was observed instead of two distinct glass transitions (Figure 5b). In the heating curve however, the broad transition appears to have two overlapping broad humps which are centered at 22 °C (T_{mid1}) and 45 °C (T_{mid2}) and they can be assigned as T_g of the poly(BA)-dominant and cholesteric polymer-dominant domains respectively. This suggests an increase in the T_g of poly(BA) and decrease in the T_g of cholesteric polymer in the semi-IPN implying presence of non-covalent interaction between the poly(BA) and the cholesteric polymer. It can be said that physically, the semi-IPN behaves more or less as a single polymer with the thermal transition smeared out over a broad range of temperature.

Mechanical Embossing of the photonic polymer film.

The semi-IPN photonic film was mechanically embossed in two steps by using a spherical glass stamp (radius of curvature = 25.8 mm) – first, above the glass transition at $T_1 = 75$ °C (i.e. $T_{high} + 21$ °C) and second, in between T_{mid1} and T_{mid2} at $T_2 = 40$ °C (i.e. $T_{mid1} + 18$ °C) (Figure 7a). At T_1 , a load of 0.7 Kg was used for embossing. Upon cooling to T_2 an extra load of 3.5 Kg was added. The film was then finally cooled below the glass transition at 0 °C with a total load of 4.2 Kg.

As the stamp used is spherical in shape, the indentation after mechanical embossing was spherical with a diameter of 1.7 mm. The central region of the indentation appeared blue in color and UV-Vis transmission spectrum showed that the reflection band has blue shifted by ~155 nm with the new position centered at $\lambda = 435$ nm (Figure 7b, c). Lower transmittance value is due to condensation of water vapor on the surface of the film at 0 °C and this was not accounted while taking baseline correction. On moving outward from the central blue embossed region, degree of compression of the pitch length decreases due to the spherical shape of the stamp and the color shifted towards higher wavelength (Figure 7b).

In another set of experiment, the photonic semi-IPN was embossed in just one step at 75 °C with a load of 5.2 Kg and was cooled directly to 0 °C. The UV-Vis study of the embossed film revealed a comparatively smaller blue shift ($\Delta\lambda_{max} = \sim 112$ nm) (Figure 17) implying the method to emboss in two steps results in more efficient compression of helical pitch. Therefore, only the investigations carried out on the two-steps embossed film will be presented in the following sections.

It should be noted here that mechanical embossing of the pure cholesteric polymer CLC-5CB resulted in a blue shift of the reflection band by only 7 nm (Figure

18). This emphasizes the role of having a second polymer network interpenetrated with the cholesteric polymer in obtaining an enormous blue shift of reflection band.

Shape recovery and optical response to temperature.

5 As the photonic film has a broad T_g , what interested us was to see the color response of the indentation as it was heated step-wise through the T_g .

The film was first heated to 8 °C. There was no visible color change even after keeping at 8 °C for 7 hrs (Figure 7b). However, UV-Vis spectrum showed a small red shift of the reflection band of the central blue region by ~10 nm after an hour and
10 keeping at 8 °C for longer than an hour hardly shifted the reflection band further. The temperature was then increased to 20 °C and within an hour, the central region of the embossed area became bluish-green ($\Delta\lambda \approx 50$ nm) and the change in color was clearly visible to the naked eye (Figure 7b, c). Heating the film to 25 °C resulted to bluish-green changing to green ($\Delta\lambda \approx 80$ nm, $t = 1$ hr). On increasing the temperature to 35
15 °C, the embossed area turned yellow ($\Delta\lambda \approx 110$ nm, $t = 1$ hr) and finally at 55 °C, it returned to the original orange ($\Delta\lambda \approx 155$ nm, $t = 1$ hr), basically covering almost the entire visible color spectrum (Figure 7b, c). Lowering the temperature at any stage did not reverse the color of the indentation to what was observed prior to increase in temperature demonstrating the characteristic of a one-way shape memory.

20 The height profile measurement of the embossed area at room temperature (25 °C) showed a maximum of 6 % indentation at the center (Figure 3d7d). This is much lower than the calculated 13 % shortening of the helical pitch of the polymer on mechanical embossing while assuming the optical response of the indentation is independent of the angle of incidence of light. This reveals that the optical response
25 seen is, in fact, largely dependent on the angle of incidence due to the curvature of the indentation.

To determine if the path followed to reach a temperature T in the regime of glass transition has an effect on the optical response of the embossed polymer film, two different heating routes were employed – (a) it was initially heated to $(T-5)$ °C and
30 later up to the desired temperature T , and (b) it was directly heated from 0 °C to T , and the amount of red shifts observed after 1 hr at T was examined (Figure 8). The samples which were pre-heated to $(T-5)$ °C were found to show slightly higher values of $\Delta\lambda$ as they have had quite some time at temperatures just lower than the target temperature to recover to their initial (non-indented) configuration. It can therefore be stated that
35 when sufficient time has not been provided for complete recovery to take place (vide

infra), they will always show a slightly higher optical response than those which are directly heated to the target temperature.

In order to understand the process of shape recovery, different embossed films were heated directly from 0 °C to different temperatures $T = 8$ to 75 °C and after
5 keeping at the desired temperatures for 7 hrs, the observed red shifts ($\Delta\lambda$) of the reflection band were recorded (Figure 9a). What is intriguing is that $\Delta\lambda$ follows a near-double sigmoidal trend - the first phase from 0 °C to 30 °C and the second phase from 30 °C to 55 °C. This may be attributed to the existence of a broad glass transition comprising of two overlapping transitions (T_{mid1} and T_{mid2}) corresponding to poly(BA)-
10 dominant and the cholesteric polymer-dominant domains (Figure 5b). In the first phase, the chains of poly(BA) gain flexibility and begin to recover to their original configuration. The cholesteric polymer chains, due to its strong non-covalent interaction with poly(BA), are compelled to recover simultaneously to certain extent. This is supported by the red shift of the reflection band of the embossed area. On raising the temperature
15 further to T_{mid2} and above, the cholesteric polymer network acquires full flexibility and consequently, complete shape recovery takes place at 55 °C.

Besides a broad temperature window of optical response, what is striking is that the response is seen at a temperature as low as 8 °C. In fact, perishable food products need storage temperature below 8 °C to prevent bacterial growth and
20 formation of toxins.²⁶⁻³⁰ On investigating the optical response of the embossed area for every 2 °C rise in temperature from 0 to 20 °C after an hour at each temperature, a steady increase in $\Delta\lambda$ can be seen (Figure 9b). Although the change in color at very low temperatures is quite small to be distinguishable to the naked eye, it can probably be discerned with a smartphone camera app.³¹

25 To study the kinetics of the shape recovery, the red shifts of the reflection band ($\Delta\lambda t$) at a specific constant temperature T ($8\text{ °C} \leq T \leq 55\text{ °C}$) with respect to the position of the reflection band at 0 °C were monitored as a function of time (Figure 10a). There is a steep increase in $\Delta\lambda t$ in the first one hour for each T . The rate then considerably slowed down. The data of Figure 10a are replotted in Figure 10b on a
30 semi-logarithmic plot to model the response of the photonic polymer film at a specific temperature. It becomes clear from this plot that the relaxation mechanism does not approach an equilibrium state at a given temperature, but rather continuously relaxes to its final fully relaxed state.

By using horizontal shifting along the time axis, i.e. using Time-Temperature-Superposition (TTS), a master curve with respect to a reference
35 temperature – here arbitrarily chosen as 20°C- was obtained (Figure 10c). The

relaxation behavior of the photonic polymer film as displayed by the master curve is described using a simple Kelvin-Voigt model, in which a spring and dashpot are modeled in parallel. The parallel spring here enforces the reversibility of the deformation and the dashpot governs the relevant time and temperature response.³²

- 5 The non-exponentiality of the response is accounted for by using the empirical Kohlrausch-Williams-Watts (KWW) equation³³⁻³⁷ which is a stretched-exponential equation, often used to describe distributions of relaxation times in a continuous rather than discrete manner, having two adjustable relaxation constants, viz. τ_{ref} and β :

$$\Delta\lambda_t/\Delta\lambda_{max}(t, T) = \left(1 - \exp\left(\frac{t_{eff}(t, T)}{\tau_{ref}}\right)^\beta\right) \quad (1)$$

- 10 Here, τ_{ref} is the average relaxation time with respect to a reference temperature and β is a parameter that describes the non-exponential behavior of the relaxation process or in other words, it is a measure of the width of the distribution of relaxation times. The best fit of the master curve was obtained when τ_{ref} has a value of 1.47×10^9 s at 20 °C, and β has a value of 0.14. As $\beta \ll 1$, the distribution of
15 relaxation times is very broad and it correlates well with the experimentally observed very broad thermal transition that the photonic semi-IPN displayed.

The TTS shift function a_T used to construct the master curve follows a standard Arrhenius type of temperature dependence (Figure 10d):

$$a_T(T) = \exp\left(\frac{\Delta U}{R}\left(\frac{1}{T} - \frac{1}{T_{ref}}\right)\right) \quad (2)$$

- 20 where ΔU is the activation energy, R the universal gas constant, T the temperature and T_{ref} a reference temperature. The activation energy, ΔU , was found to be 432 kJ mol⁻¹; a rather large value indicating that the influence of temperature is (much) stronger compared to time.

- The effective time, t_{eff} , required for the recovery of the embossed area to
25 different degrees is given by:

$$t_{eff}(t, T) = \int_0^t a_T^{-1}(T) dt' \quad (3)$$

- As can be seen from Figure 9c, at 20 °C, it will take ~ 1015 s for $\frac{\Delta\lambda_t}{\Delta\lambda_{max}}$ to reach the value 1. This implies that the embossed photonic film will take more than 30 million years to recover completely to the original configuration when stored at 20 °C. It
30 can, therefore, be said that the non-equilibrium configurations the embossed film attains in the regime of glass transition are quasi-stable in nature. So, the shape recovery basically takes place in multi-stages with partial recovery at each recovery

temperature of the broad thermal transition. The quasi-stable intermediate configurations display distinct optical response in measurable time scale, thereby exerting the ability of the photonic film to act as an optical time-temperature integrator in the broad temperature window of 0 to 55 °C. However as the effect of time on the response is small compared to temperature, it may be difficult to visualize the color change by the naked eye for different times, especially after 1 hr, when the rate of optical change had slowed down considerably –say between 2 and 4hr at a particular temperature. The semi-IPN photonic films which we have fabricated are, therefore, more attractive for temperature sensor applications.

10

Conclusion

A photonic polymer film with a broad glass transition temperature from 10 to 54 °C has been fabricated from a semi-interpenetrating network of a cholesteric polymer and poly(benzyl acrylate). The mechanically embossed photonic film exhibits shape memory effect and displays multiple intermediate quasi-stable shapes of distinct color in the temperature window of 0 to 55 °C in measurable time scale, making this material attractive for application as optical temperature sensors. If the small optical response could be deciphered with a smartphone camera app, they can be of interest as time-temperature integrators for applications such as smart packaging labels to record thermal history of perishable food products. A more balanced sensitivity to time and temperature would, however, be a better approach and this could possibly be achieved by further tuning the chemistry of the semi-interpenetrating polymer network.

15

Supporting Information is provided in appendix C: DSC, FT-IR, TGA and UV-Vis measurements, TEM images and experimental details. This material is available free of charge via the Internet at <http://pubs.acs.org>.

20

References

- (1) Berg, G. J.; McBride, M. K.; Wang, C.; Bowman, C. N. *Polymer (Guildf)*. 2014, 55 (23), 5849.
- (2) Hu, J.; Zhu, Y.; Huang, H.; Lu, J. *Prog. Polym. Sci.* 2012, 37 (12), 1720.
- (3) Sun, L.; Huang, W. M.; Ding, Z.; Zhao, Y.; Wang, C. C.; Purnawali, H.; Tang, C. *Mater. Des.* 2012, 33 (1), 577.
- (4) Meng, H.; Li, G. *Polymer (Guildf)*. 2013, 54 (9), 2199.
- (5) Xie, T. *Polymer (Guildf)*. 2011, 52 (22), 4985.
- (6) DiOrio, A. M.; Luo, X.; Lee, K. M.; Mather, P. T. *Soft Matter* 2011, 7 (1), 68.
- (7) Behl, M.; Lendlein, A. *J. Mater. Chem.* 2010, 20 (17), 3335.

35

- (8) Qin, H.; Mather, P. T. *Macromolecules* 2009, 42 (1), 273.
- (9) Lendlein, A.; Behl, M. *Adv. Sci. Technol.* 2008, 54, 96.
- (10) Ge, J.; Yin, Y. *Angew. Chem. Int. Ed.* 2011, 50 (7), 1492.
- (11) Davies, D. J. D.; Vaccaro, A. R.; Morris, S. M.; Herzer, N.; Schenning, A. P. H.
5 J.; Bastiaansen, C. W. M. *Adv. Funct. Mater.* 2013, 23 (21), 2723.
- (12) Fang, Y.; Ni, Y.; Leo, S.-Y.; Taylor, C.; Basile, V.; Jiang, P. *Nat. Commun.* 2015,
6 (May), 7416.
- (13) Fang, Y.; Ni, Y.; Choi, B.; Leo, S. Y.; Gao, J.; Ge, B.; Taylor, C.; Basile, V.;
Jiang, P. *Adv. Mater.* 2015, 27 (24), 3696.
- 10 (14) Fang, Y.; Leo, S. Y.; Ni, Y.; Yu, L.; Qi, P.; Wang, B.; Basile, V.; Taylor, C.;
Jiang, P. *Adv. Opt. Mater.* 2015, 3 (11), 1509.
- (15) Fang, Y.; Ni, Y.; Leo, S.-Y.; Wang, B.; Basile, V.; Taylor, C.; Jiang, P. *ACS
Appl. Mater. Interfaces* 2015, 151008093456008.
- (16) Xie, T. *Nature* 2010, 464 (7286), 267.
- 15 (17) Zhao, Q.; Behl, M.; Lendlein, A. *Soft Matter* 2013, 9 (6), 1744.
- (18) Li, J.; Liu, T.; Xia, S.; Pan, Y.; Zheng, Z.; Ding, X.; Peng, Y. *J. Mater. Chem.*
2011, 21 (33), 12213.
- (19) Stumpel, J. E.; Gil, E. R.; Spoelstra, A. B.; Bastiaansen, C. W. M.; Broer, D. J.;
Schenning, A. P. H. *J. Adv. Funct. Mater.* 2015, 25 (22), 3314.
- 20 (20) Mulder, D.-J.; Schenning, A.; Bastiaansen, C. *J. Mater. Chem. C* 2014, 2 (33),
6695.
- (21) White, T. J.; McConney, M. E.; Bunning, T. J. *J. Mater. Chem.* 2010, 20 (44),
9832.
- (22) Carlton, R. J.; Hunter, J. T.; Miller, D. S.; Abbasi, R.; Mushenheim, P. C.; Tan,
25 L. N.; Abbott, N. L. *Liq. Cryst. Rev.* 2013, 1 (1), 29.
- (23) Poly(benzyl acrylate)
<http://polymerdatabase.com/polymers/polybenzylacrylate.html>.
- (24) Spahn, P.; Finlayson, C. E.; Etah, W. M.; Snoswell, D. R. E.; Baumberg, J. J.;
Hellmann, G. P. *J. Mater. Chem.* 2011, 21 (24), 8893.
- 30 (25) Chang, C.-K.; Kuo, H.-L.; Tang, K.-T.; Chiu, S.-W. *Appl. Phys. Lett.* 2011, 99
(7), 73504.
- (26) De Jonghe, V.; Coorevits, A.; Van Hoorde, K.; Messens, W.; Van Landschoot,
A.; De Vos, P.; Heyndrickx, M. *Appl. Environ. Microbiol.* 2011, 77 (2), 460.
- (27) Smadi, H.; Sargeant, J. M.; Shannon, H. S.; Raina, P. J. *Epidemiol. Glob.
35 Health* 2012, 2 (4), 165.
- (28) Millogo, V.; Sissao, M.; Gisèle, A.; Anago, S.; Anicet, G. 2015, 2 (1), 104.

- (29) Lidster, P. D.; Hildebrand, P. D.; Brard, L. S.; Porritt, S. W. Commercial storage of fruits and vegetables; 1988.
- (30) Kerbel, E. Commer. Storage Fruits , Veg. , Flor. Nurs. Stock. 2016, No. 66, 224.
- (31) El Kaoutit, H.; Estévez, P.; García, F. C.; Serna, F.; García, J. M. Anal. Methods
5 2013, 5 (1), 54.
- (32) Ward, I. M.; Sweeney, J. An Introduction to the Mechanical Properties of Solid Polymers, 2nd ed.; John Wiley and sons: Chichester, 2004.
- (33) Kohlrausch, F. Ann. der Phys. und Chemie. 1866, 128 (5), 1.
- (34) Kohlrausch, F. Ann. der Phys. und Chemie. 1866, 128 (5), 207.
- 10 (35) Kohlrausch, F. Ann. der Phys. und Chemie. 1866, 128 (5), 399.
- (36) Williams, G.; Watts, D. C. Trans. Faraday Soc. 1970, 66 (1), 80.
- (37) Matsuoko, S. Relaxation Phenomena in Polymers; Hanser Publishers: Munich, 1992.

15 **Appendix C – Supporting Information: A Photonic Shape Memory Interpenetrating Polymer Network with a Broad Temperature and Color Response.**

Experimental Details

20 Materials: RM 257, RM 105 and 5CB were obtained from Merck. LC756 was bought from BASF. Benzyl acrylate was purchased from Sigma Aldrich. Irgacure 651 was from CIBA. Tetrahydrofuran was obtained from Biosolve.

Equipments: Photopolymerization was carried out with Omnicure series 2000 EXFO lamp. UV-Visible spectra of the photonic film were measured in Shimadzu UV-3102 PC
25 spectrophotometer. Differential scanning calorimetry was performed in TA DSC Q1000. Thermogravimetric curve was measured in TA TGA Q500. FT-IR spectra were recorded using Varian 670 FT-IR spectrometer with slide-on ATR (Ge). Mechanical Embossing was carried out in a DACA Tribotrak with a spherical glass stamp of diameter 25.8 mm. Ocean Optics UV-Visible spectrophotometer HR2000+ mounted on
30 a DM6000 M microscope from Leica microsystems was used for monitoring the shape recovery of embossed films. T95-PE from Linkam Scientific was used to study temperature dependent transmission spectra. Images of the embossed film were captured using Leica M80 stereomicroscope. Height profile was measured using Bruker DektakXTL profilometer.

35 Preparation of photonic polymer film: 1g of mesogen mixture consisting of 29 wt. % RM257, 35 wt. % RM105, 30 wt. % 5CB, 5 wt. % LC 756 and 1 wt. % Irgacure 651 was

dissolved in 4 mL of tetrahydrofuran to form a homogeneous solution. The solvent was later evaporated by heating at 75 °C to obtain the cholesteric liquid crystalline (CLC) mixture. The CLC mixture was then filled in a polyimide rubbed cells with 70 µm spacer at 40 °C followed by photopolymerization by irradiating UV light (48 mW cm⁻² intensity in the range 320-390 nm) for 5 min. The cell was opened to obtain a free standing cholesteric polymer film. It was then treated with THF and dried, first at room temperature and then at 75 °C, after which the polymer film was exposed to benzyl acrylate mixed with 1 wt. % of Irgacure 651 for 12 hr. After wiping out excess benzyl acrylate, it was photopolymerized in N₂ atmosphere by shining UV light for 10 min each on both the sides of the polymer film. The process was repeated again to incorporate high amount of benzyl acrylate in the system.

The results are shown in figures 11-18.

Appendix D – Temperature-responsive reflective coatings

Stimulus-responsive color reflective materials based on cholesteric liquid crystals are interesting for decorative purposes, sensors and smart window applications. In most cases these responsive systems make use of low molecular weight liquid crystals (LMWLCs) to provide a switchable LC medium. Since LMWLCs are volatile, these systems are limited to closed cells and not suitable for coating applications. In this work we present a route towards temperature-responsive coatings based on side chain liquid crystalline polysiloxanes (SCLCP). The SCLCP is combined with reactive mesogens to form an interpenetrating network (IPN) after coating into a film and subsequent polymerization. The reflection band (colour) shifts upon heating.

Figure 19 shows IPN formed from SCLCP combined with reactive mesogens is coated into film and subsequently polymerized.

Figure 20 shows siloxane liquid crystal polymer + reactive mesogens composition. With reference to Appendix A, the molecular structures from bottom to top refer to SCLCP, RM-4, RM-1.

Figure 21 B: is the same as Figure 3.

Appendix E – Semi-IPNs of a densely crosslinked cholesteric network and a siloxane liquid crystal polymer.

Semi-interpenetrating networks were prepared by mixing reactive mesogens (RMs) with a siloxane liquid crystal polymer (SiLCP). The chemical structures are shown in the appendix. The 0% mixture is based on the RM mixture reported by Davies et al, Adv. Funct. Mater. 2013, 23, 2723–2727. SiLCP was added in

various wt%, while the relative wt.% of the RM components was kept constant. No macrophase separation was observed for any of the mixtures.

Table 1. Cholesteric mixture formulation (wt. %)

| | 0% | 10% | 20% | 30% | 50% | 70% | 100% |
|----------|------|------|------|------|------|------|------|
| SiLCP | 0,0 | 9,3 | 19,8 | 28,7 | 50,1 | 69,5 | 100 |
| 6OBA | 21,7 | 19,3 | 16,9 | 14,6 | 10,2 | 5,8 | 0 |
| 6OBA-M | 21,9 | 20,6 | 17,2 | 14,9 | 10,3 | 5,7 | 0 |
| LC1516 | 37,8 | 33,5 | 29,0 | 25,2 | 18,7 | 10,6 | 0 |
| RM 82 | 12,8 | 11,3 | 11,0 | 10,7 | 6,2 | 3,5 | 0 |
| LC756 | 4,5 | 4,7 | 4,5 | 4,6 | 3,7 | 3,9 | 0 |
| Irga 369 | 0,9 | 0,8 | 1,1 | 0,8 | 0,7 | 0,8 | 0 |
| BHT | 0,5 | 0,5 | 0,5 | 0,5 | 0,2 | 0,2 | 0 |
| Total | 100 | 100 | 100 | 100 | 100 | 100 | 100 |

5 The thermal properties of the monomeric mixtures were investigated by differential scanning calorimetry (Figure 22). Upon addition of SiLCP, the clearing temperature of the cholesteric phase is reduced. A minimum is observed at 30% SiLCP fraction (33°C). An additional phase transition is found at lower temperatures.

10 The monomeric mixtures were subsequently photopolymerised, and the thermal properties of the were investigated using DSC. Glass transitions were observed as indicated in Figure 23. At 0%, the T_g occurs at 48°C and is approximately 4° broad (indicated by the black line). At 10%, the T_g is reduced to 27 °C and it is significantly broadened (9° C). This indicates molecular mixing of RM and SiLCP components. The broadening of the At higher SiLCP fractions, two distinct T_gs are
15 observed, which correspond to neat RM and neat SiLCP, respectively. The presence of two distinct T_gs suggests microphase separation of the RM and SiLCP components.

20 The 10% formulation was used to construct a temperature sensor (Figure 24). A thin film (10 micron thickness) was coated on a glass plate containing a rubbed poly(imide) surface, and subsequently UV-polymerised, to result in a red-reflecting polymer film. The polymer film was hot-embossed at 70°C using a 2.5 kg load consisting of a spherical stamp. The film was cooled to room temperature under continuous load to result in a green-reflecting area (indicated by the arrow). When

heated to 50°C for 10 minutes, the embossed area returned to the original red-reflecting colour.

CLAIMS

1. Photonic time-temperature sensor consisting of an embossed cholesteric liquid crystalline polymer network and a secondary polymer.
5
2. Photonic time-temperature sensor according to claim 1 in which the secondary polymer is orthogonal and is not covalently attached to the cholesteric liquid crystalline polymer network, but physically interpenetrated therein.
10
3. Photonic time-temperature sensor according to claim 1 or claim 2 in which the secondary polymer is either crystalline in nature or liquid crystalline or amorphous in nature.
- 15 4. Photonic time-temperature sensor according to one or more of the preceding claims in which the material properties as to chemistry and/or volume fraction of the secondary polymer can suitably be changed.
- 20 5. Photonic time-temperature sensor according to one or more of the preceding claims in which the material properties of the interpenetrating network have suitably been tuned.
- 25 6. Photonic time-temperature sensor according to one or more of the preceding claims in the form of a single layer of plastic or an adhesive sticker which can suitably be printed, respectively put on packaging containers.
- 30 7. Photonic time-temperature sensor according to claim 6 in which the plastic is selected from the group consisting of polysiloxanes, acrylics, polyethers, polyesters, polyolefins.
8. Photonic time-temperature sensor according to claim 7 in which the plastic is a polyolefin, a polyester, a polyimide, a polyamide and the like.
- 35 9. A plastic strip which contains a photonic time-temperature sensor according to one or more of the preceding claims 1-9 inclusive.

10. A time-temperature indicating device or product other than a plastic strip containing a photonic time-temperature sensor according to one or more of the preceding claims 1-9 inclusive.
- 5 11. Food sensor for checking freshness of the food containing or consisting of a photonic time-temperature indicator according to to one or more of the preceding claims.
- 10 12. Process for preparing a time-temperature indicating device or product according to one or more of the preceding claims consisting of the following steps.
- 15 1. Preparing a formulation consisting of reactive liquid crystal mesogens and a compatible secondary polymer. This polymer has a suitably low glass transition temperature, for example but not limited to a poly(dimethylsiloxane) or a derivative thereof.
 2. Printing a thin layer (3-20 μm) of said formulation onto a substrate with a (rubbed) alignment layer by conventional LC processing techniques (screen, flexographic, inkjet printing, bar-coating, slid die coating etc).
 - 20 3. Polymerizing the layer, for instance, by UV-irradiation to form the interpenetrating network.
- Mechanical embossing of the layer at an appropriate temperature (-20 to 60°C) to induce the photonic memory effect.

25

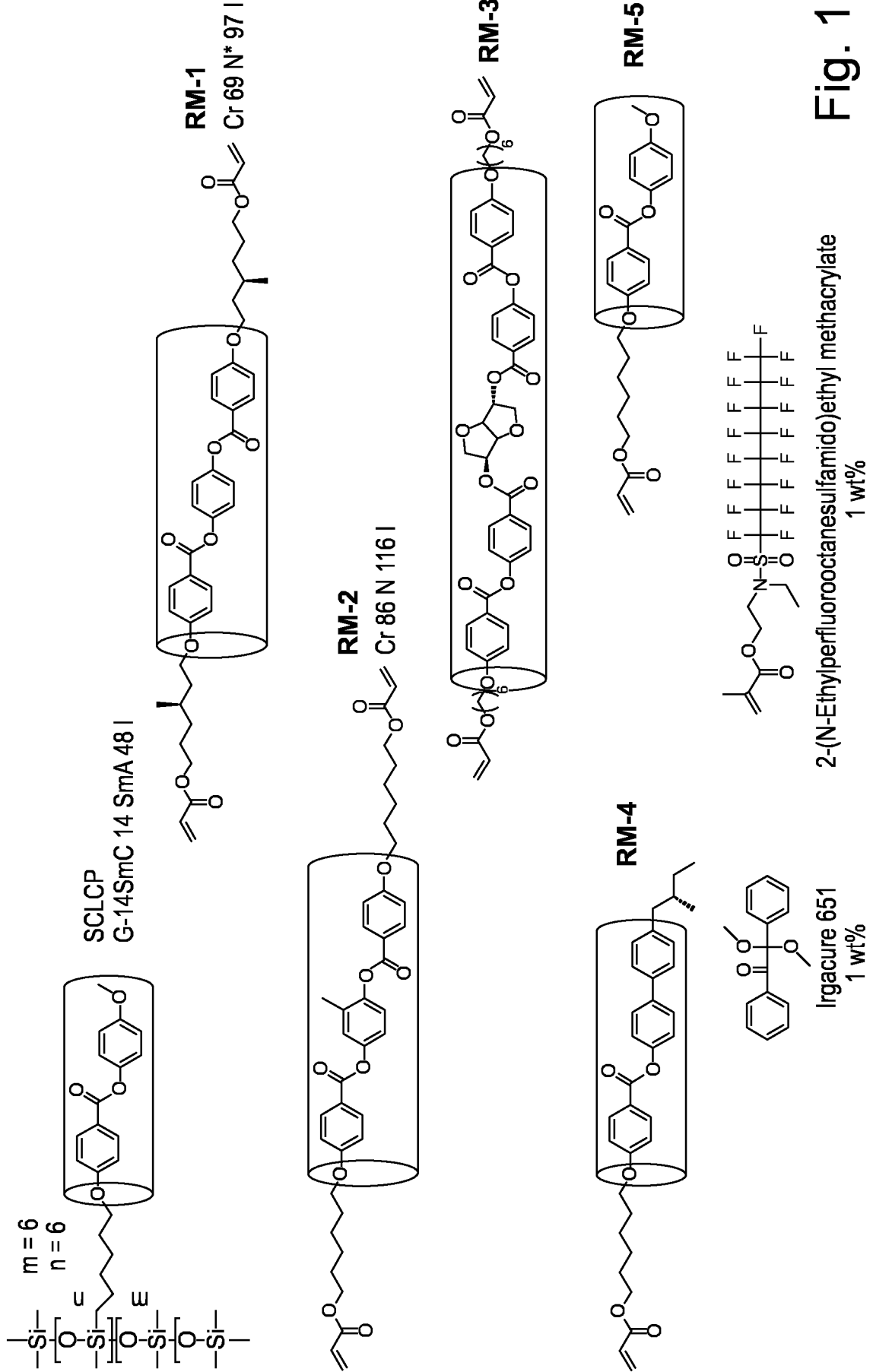


Fig. 1

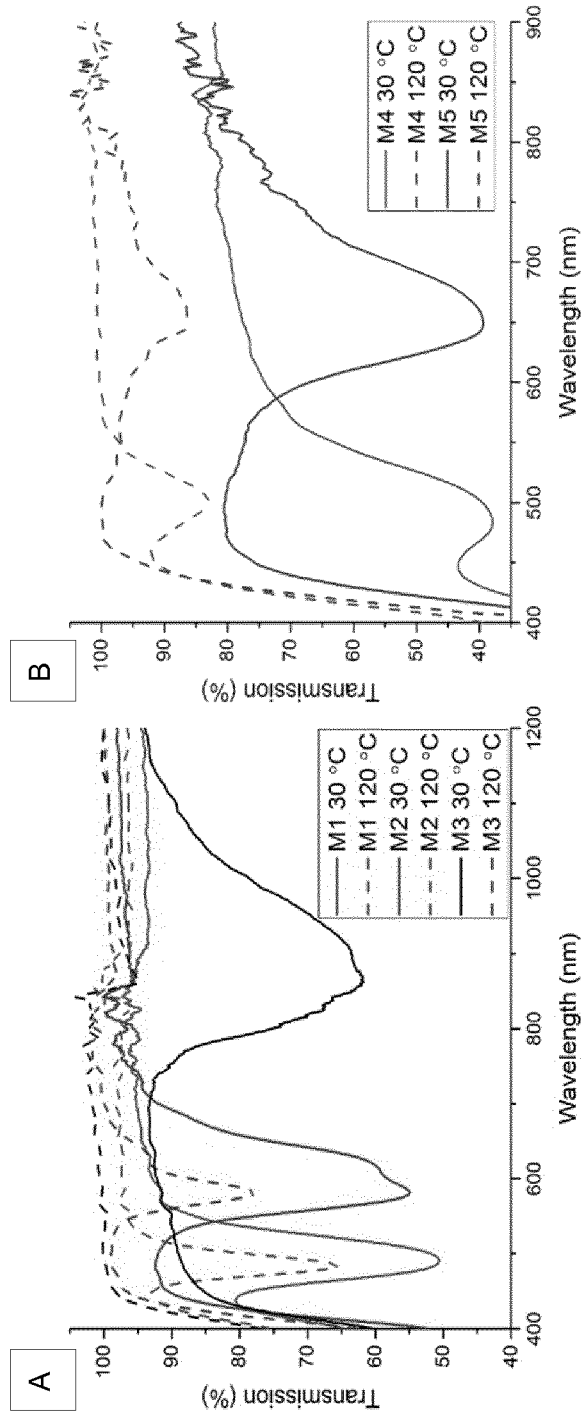


Fig. 2

3/24

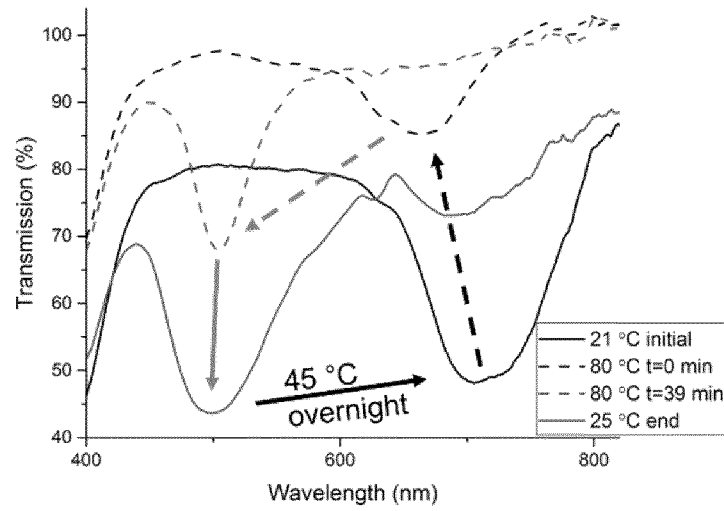


Fig. 3

4/24

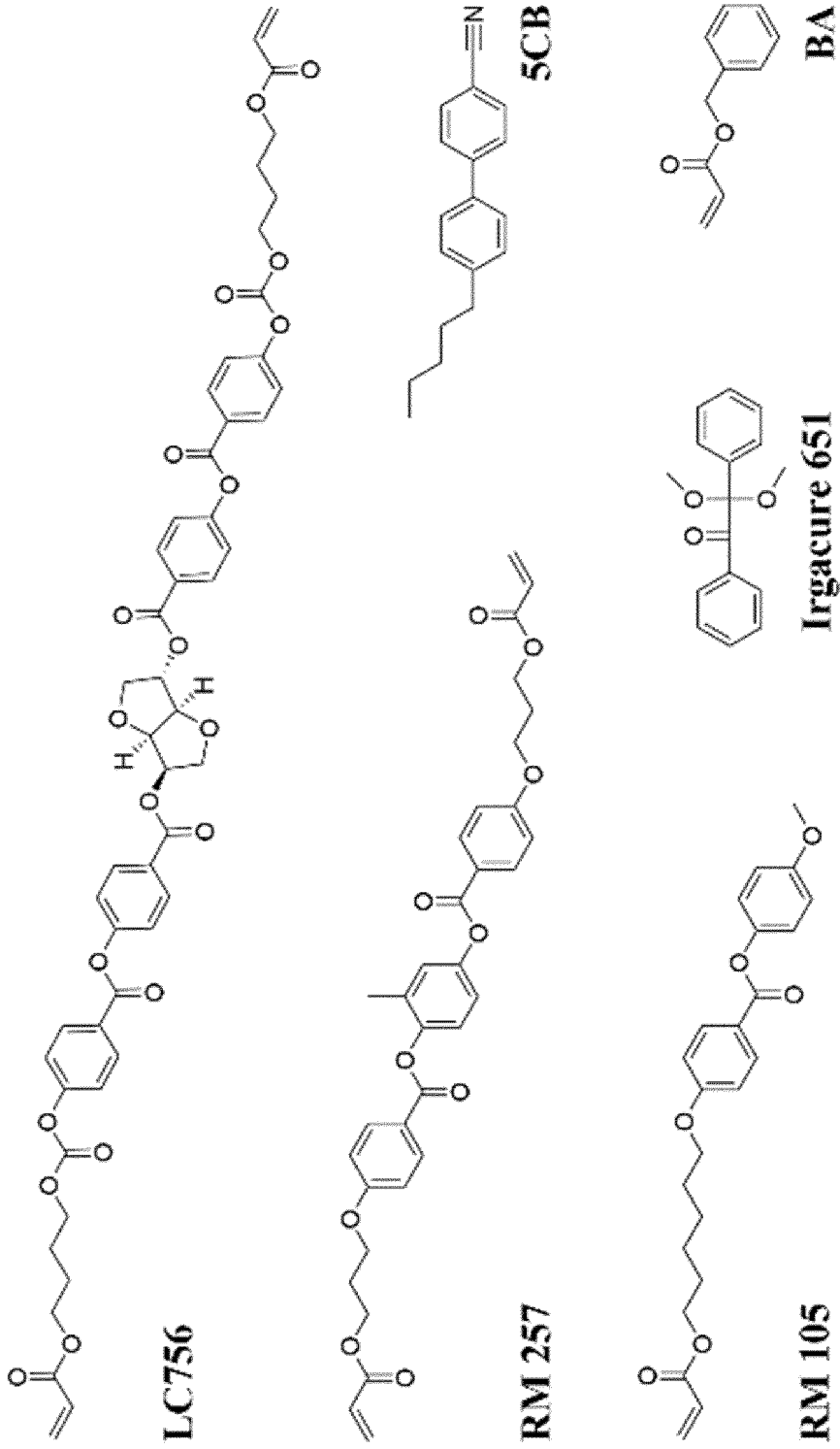


Fig. 4

5/24

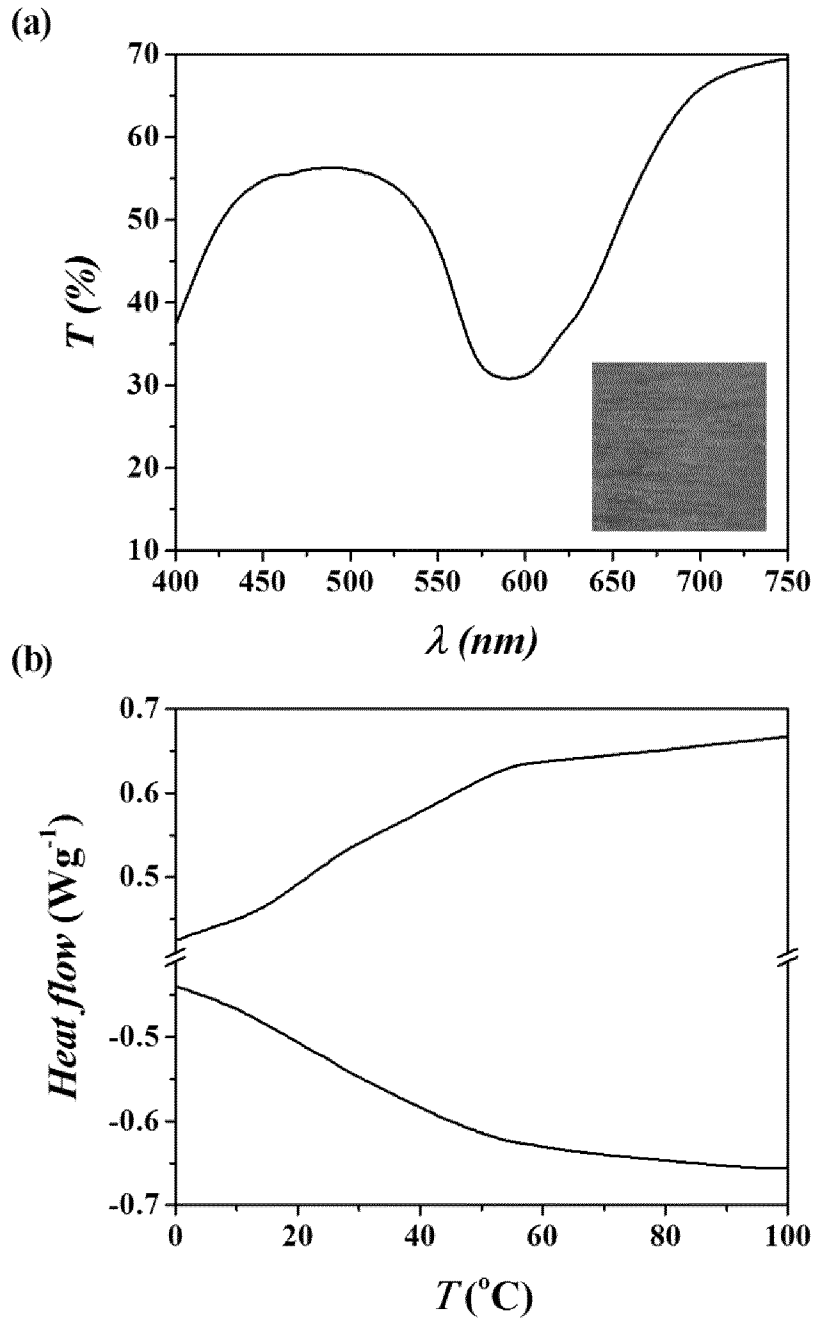


Fig. 5

6/24

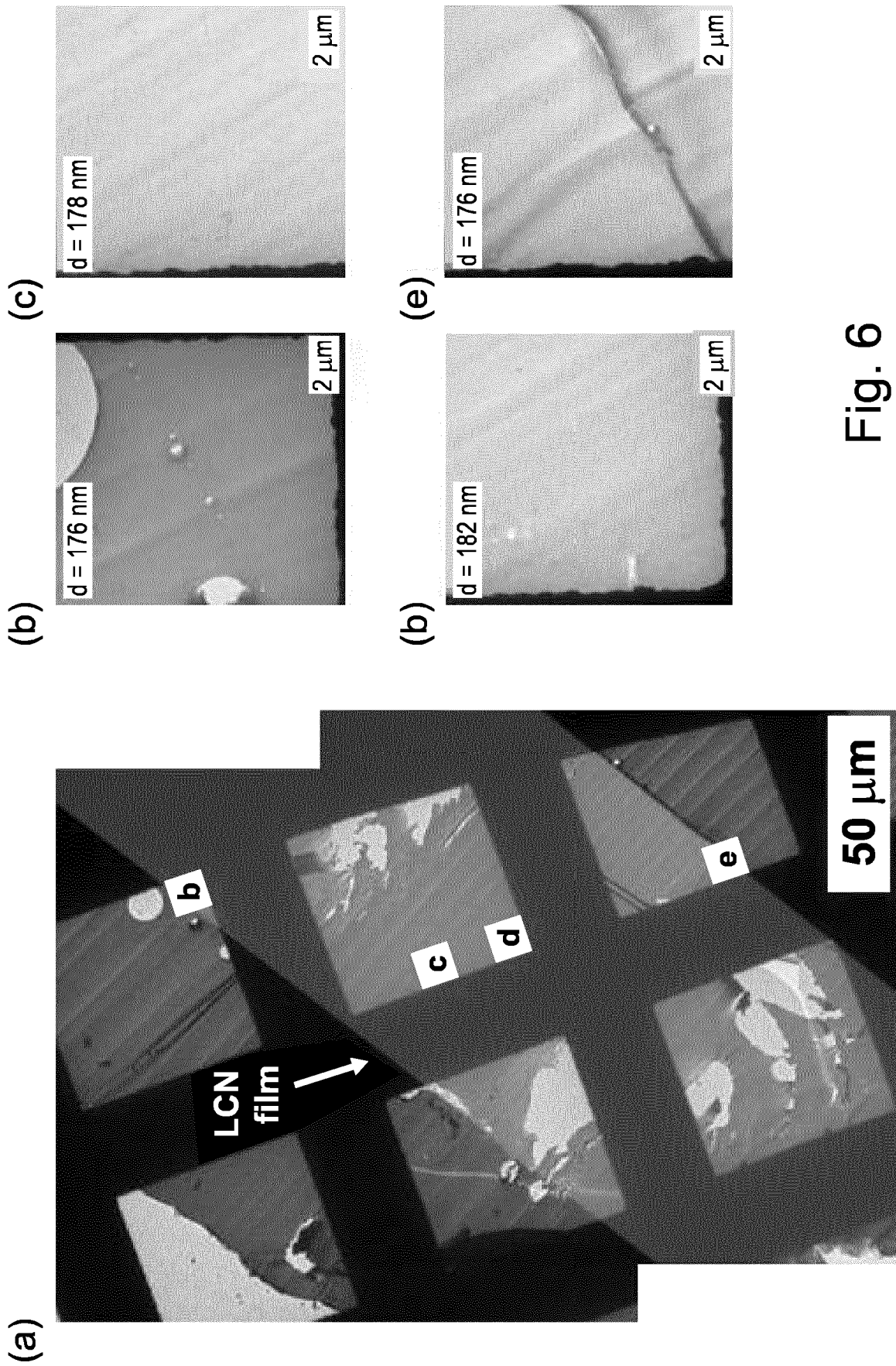


Fig. 6

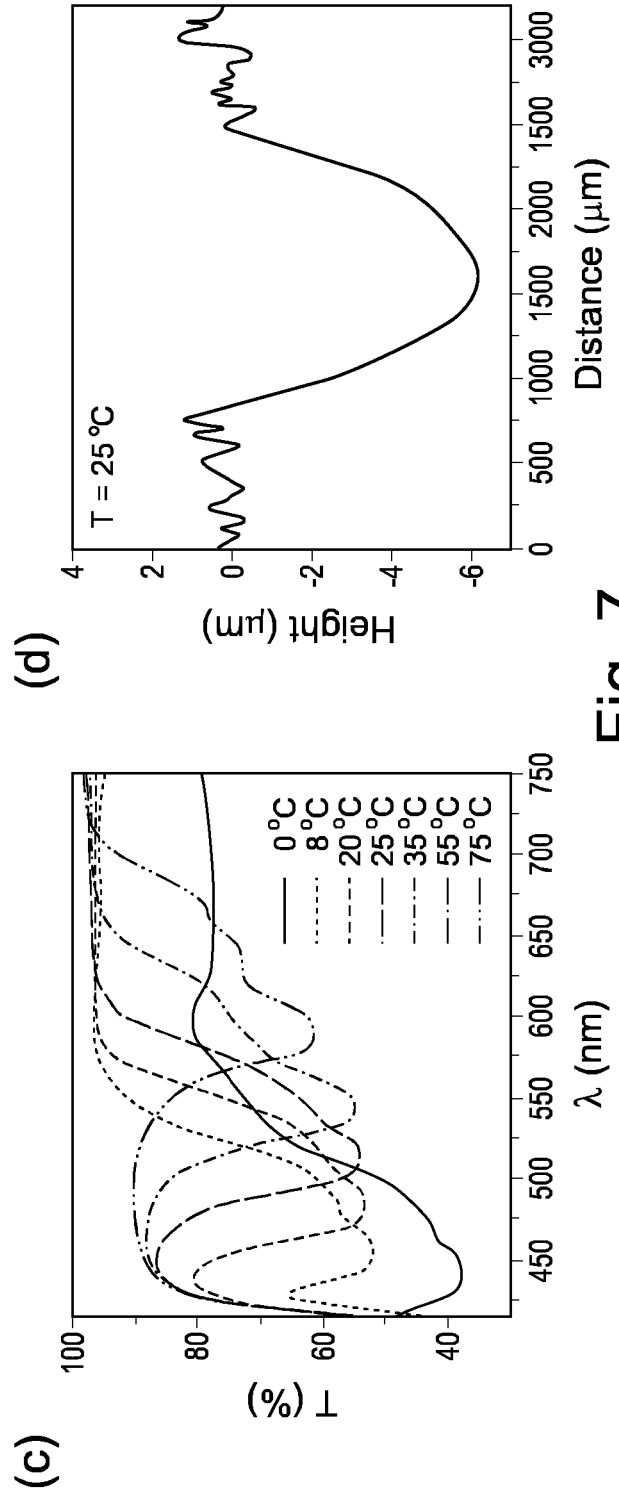
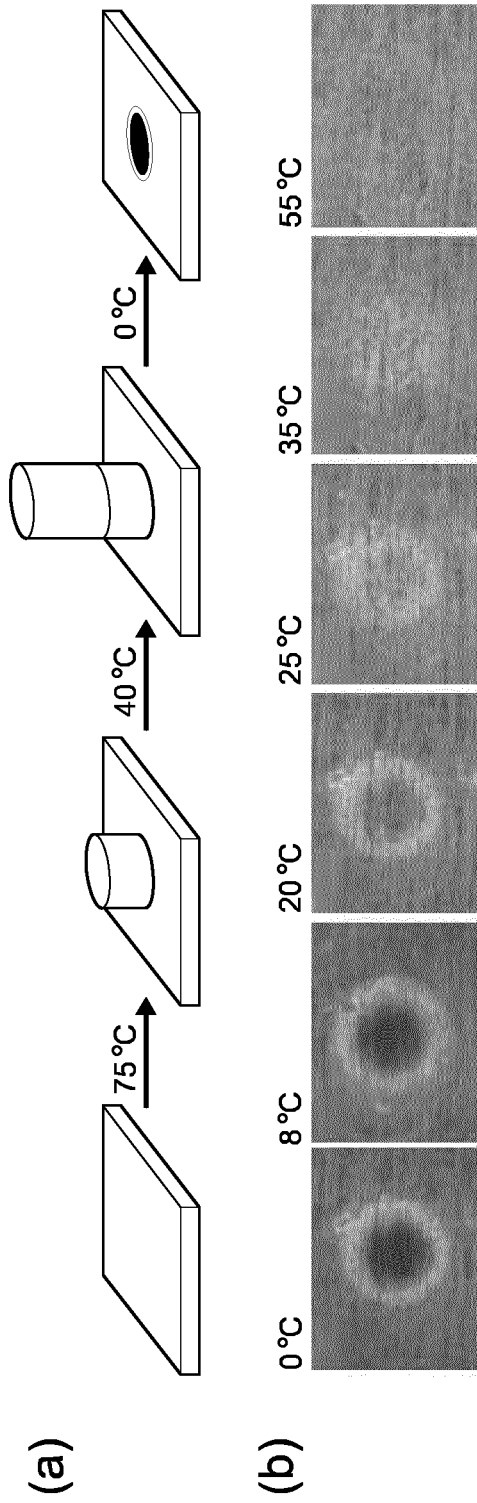


Fig. 7

8/24

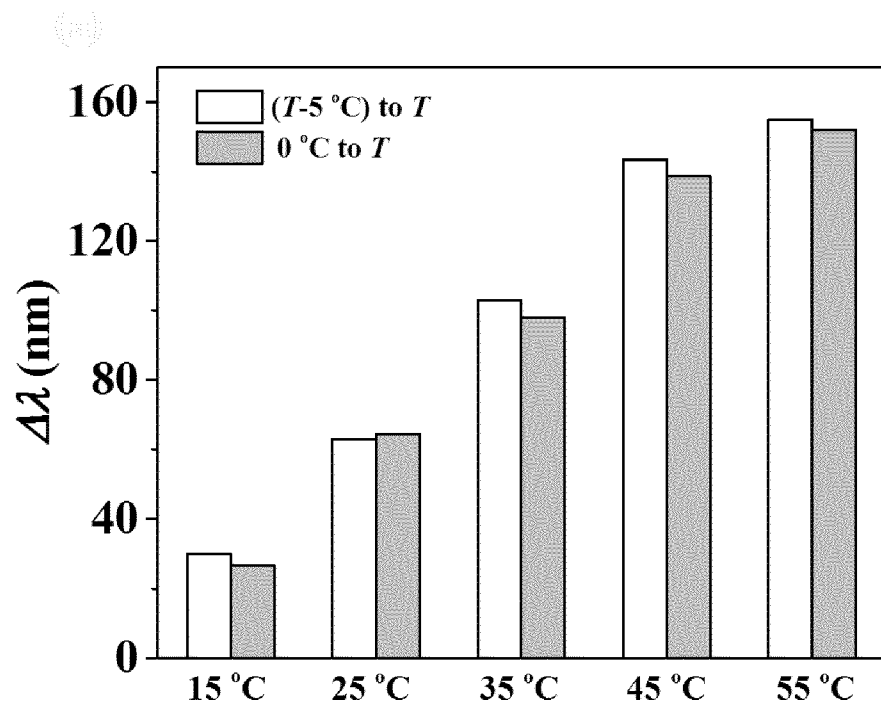


Fig. 8

9/24

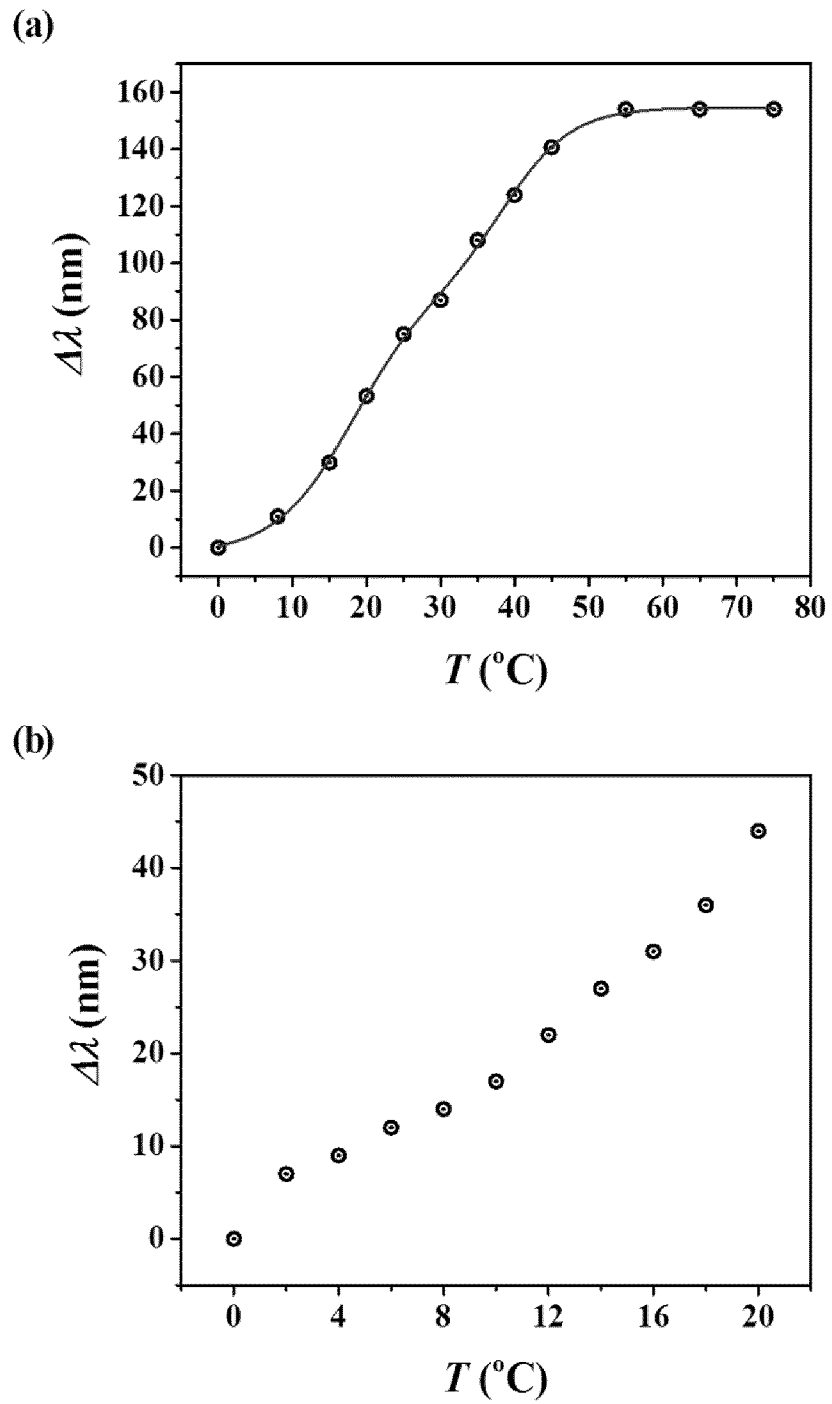


Fig. 9

10/24

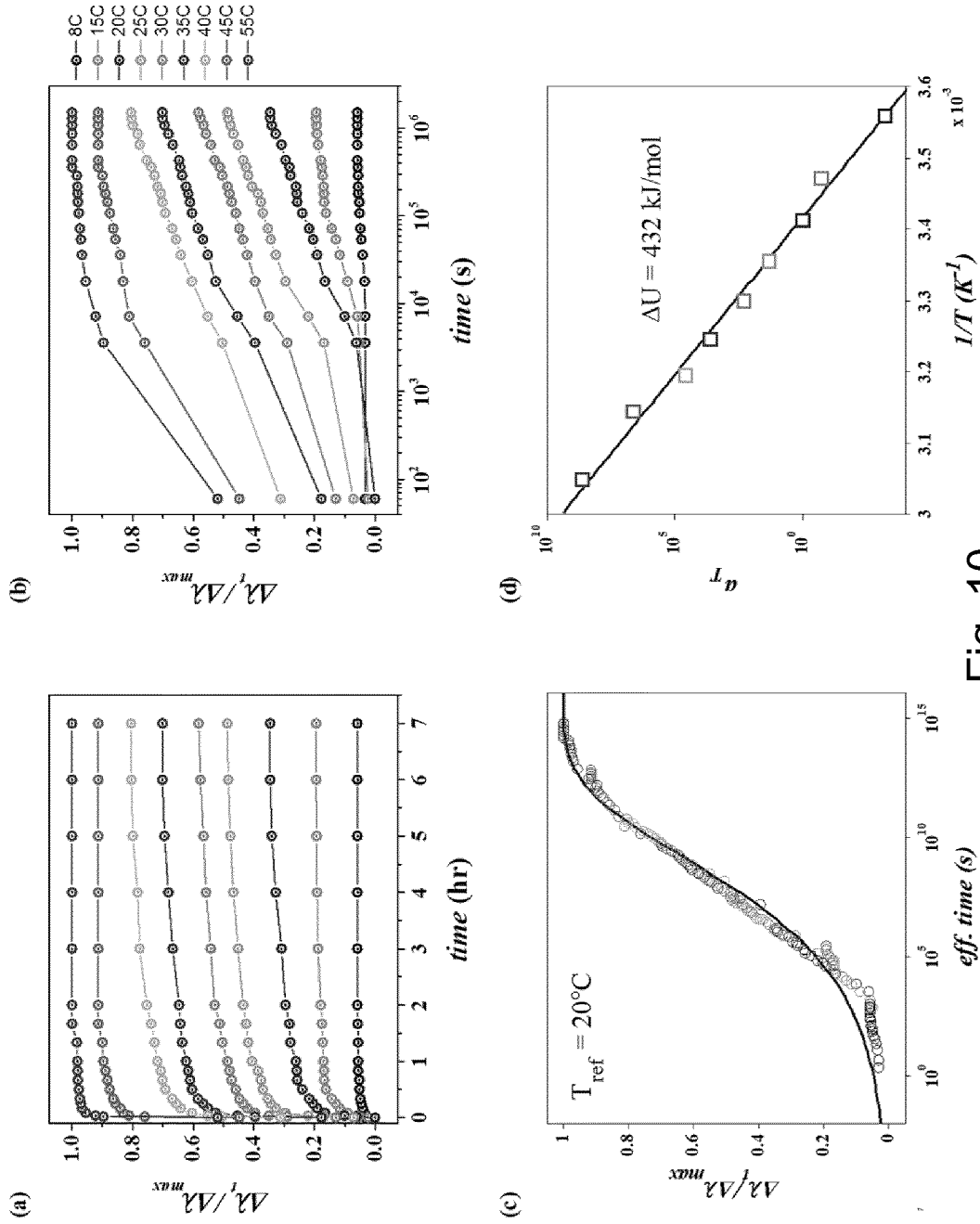


Fig. 10

11/24

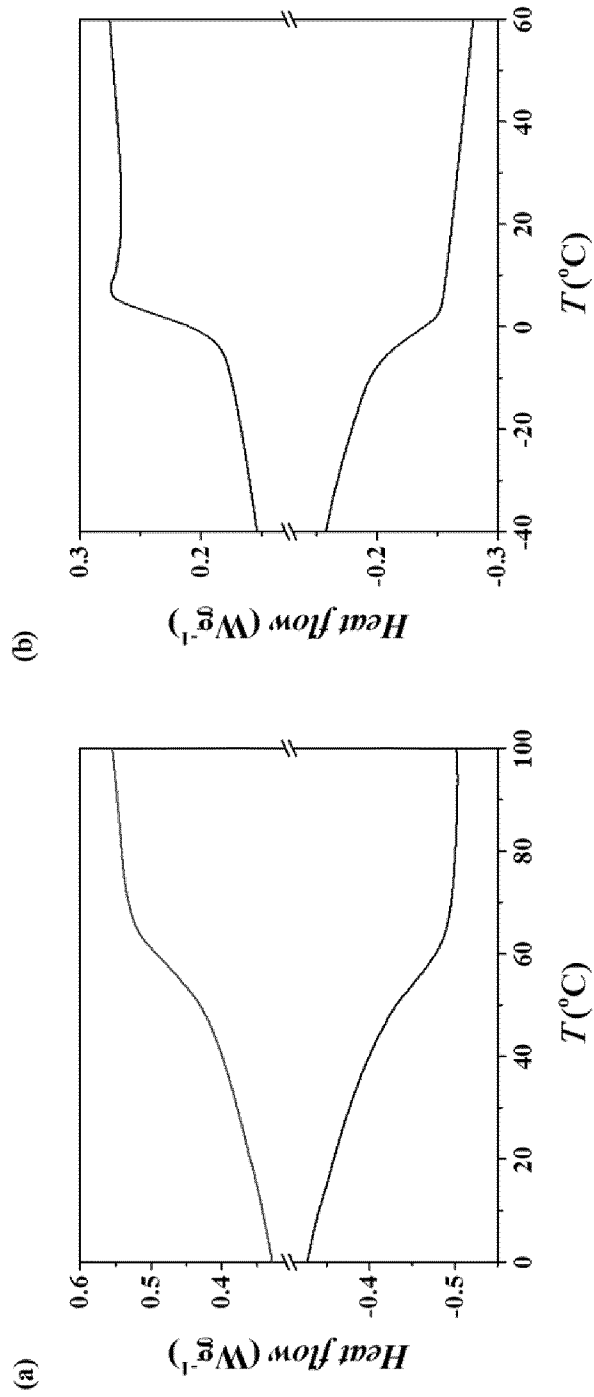


Fig. 11

12/24

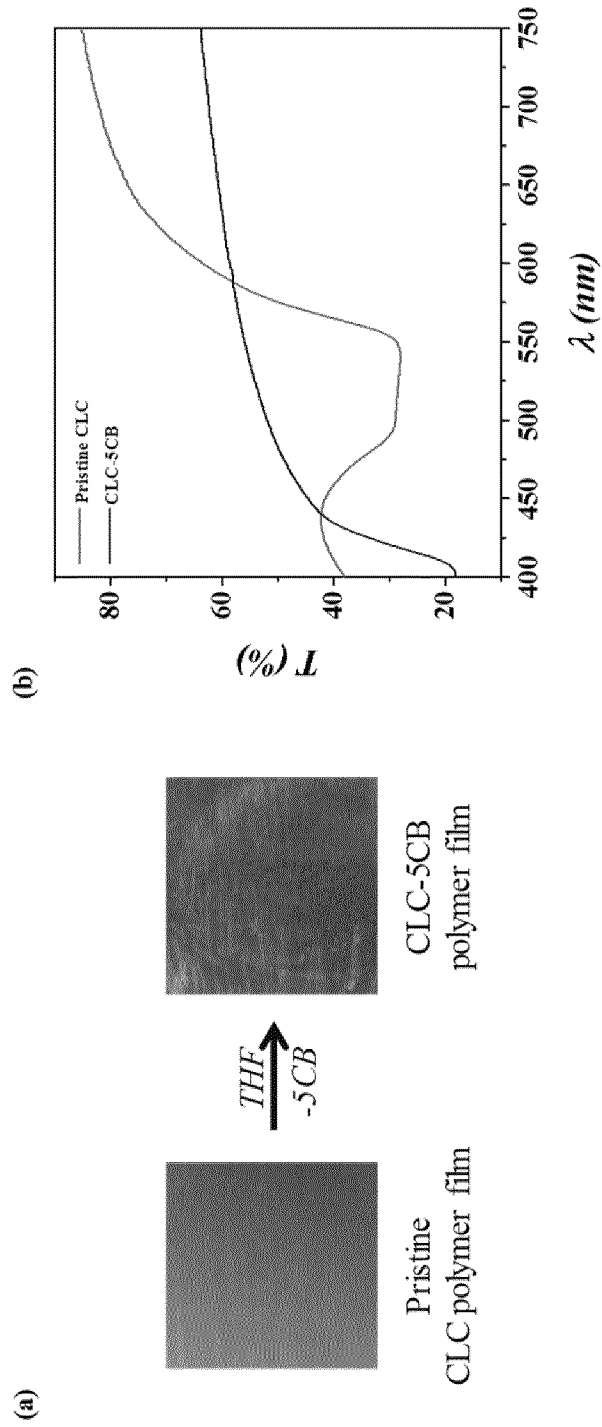


Fig. 12

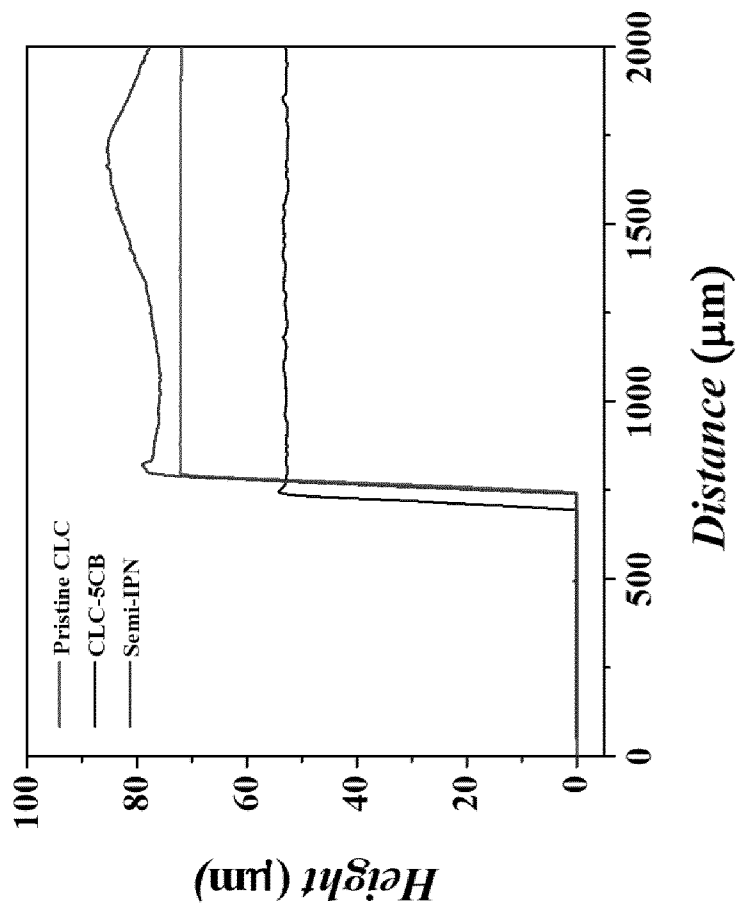


Fig. 13

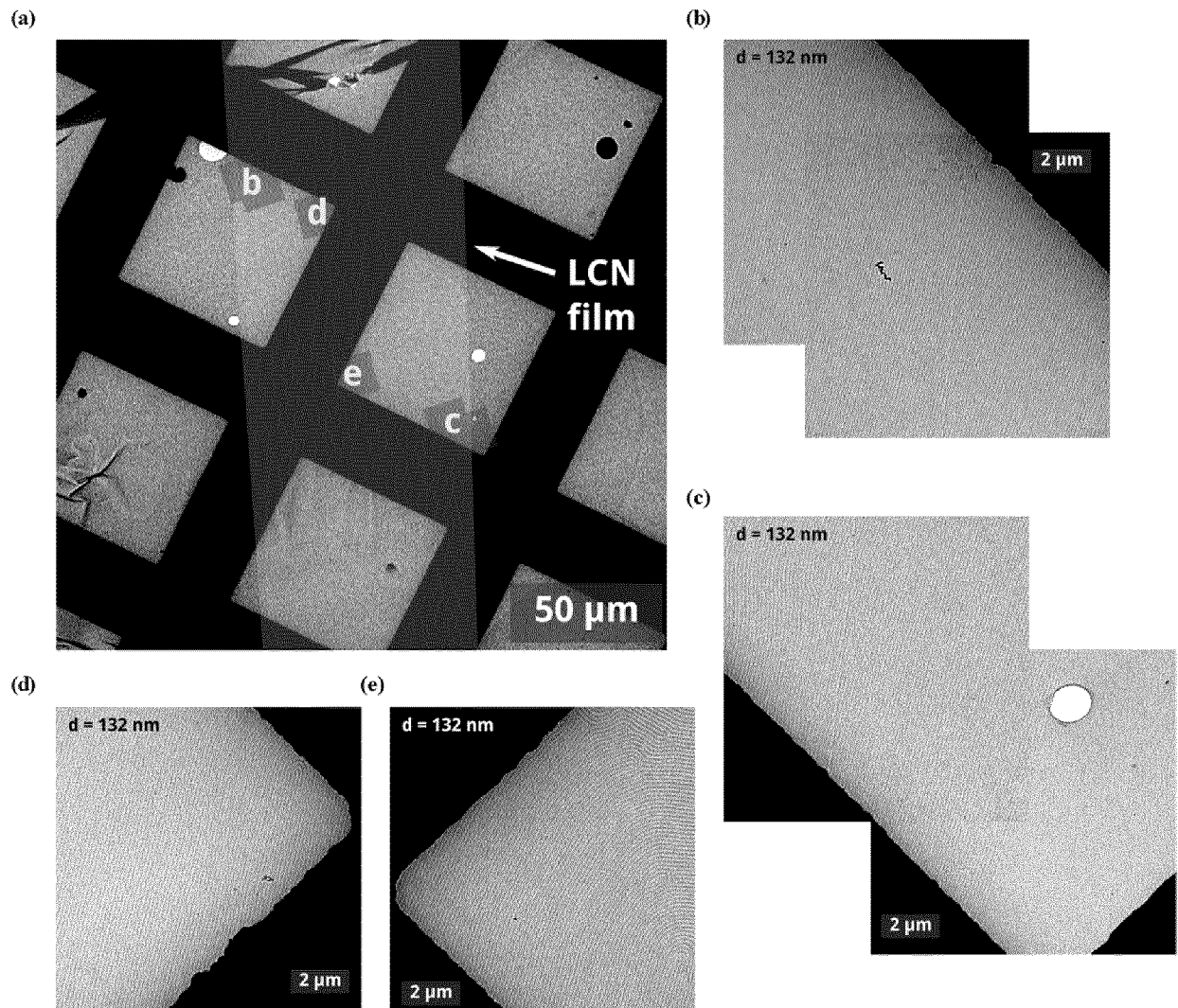


Fig. 14

15/24

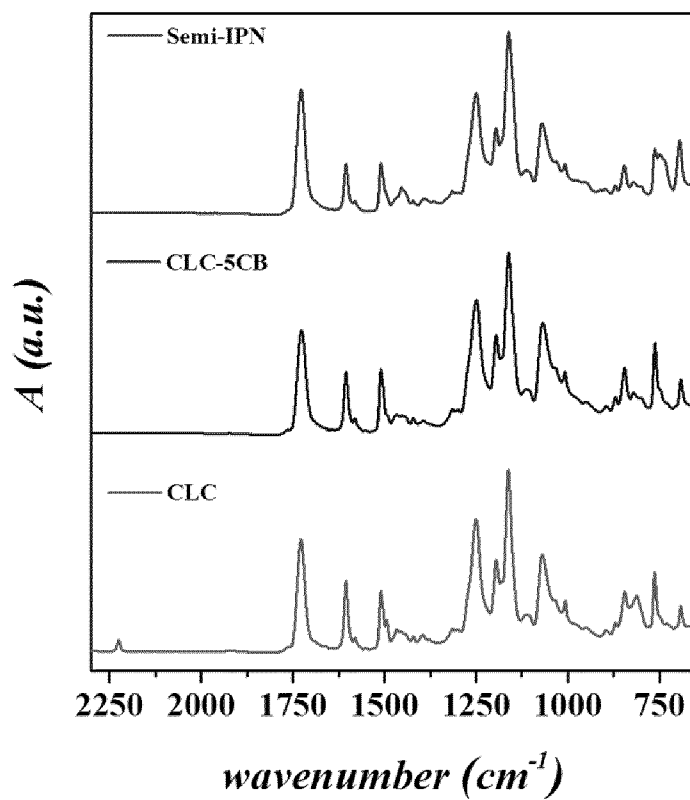


Fig. 15

16/24

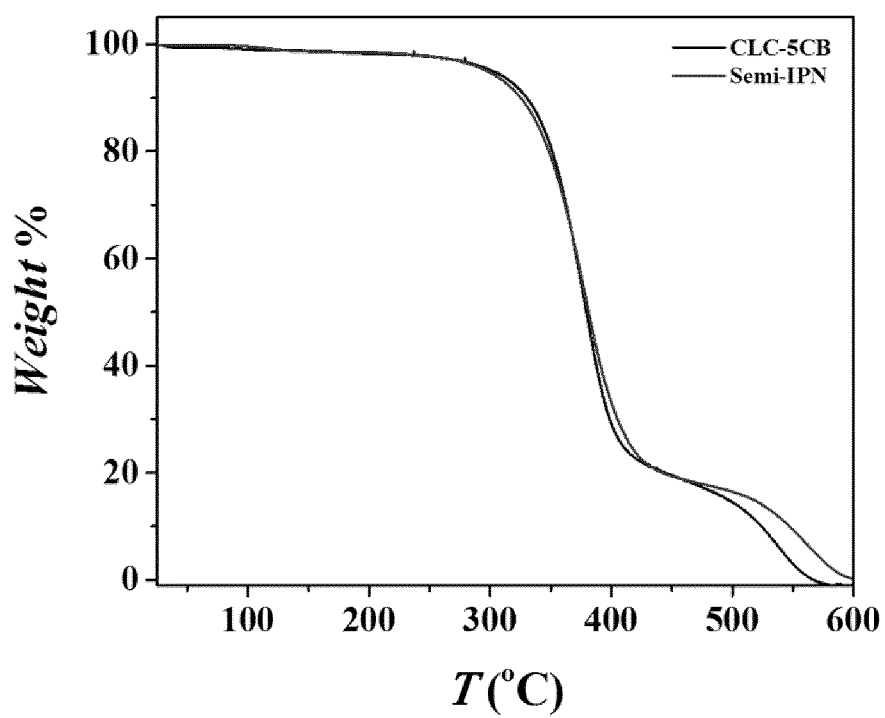


Fig. 16

17/24

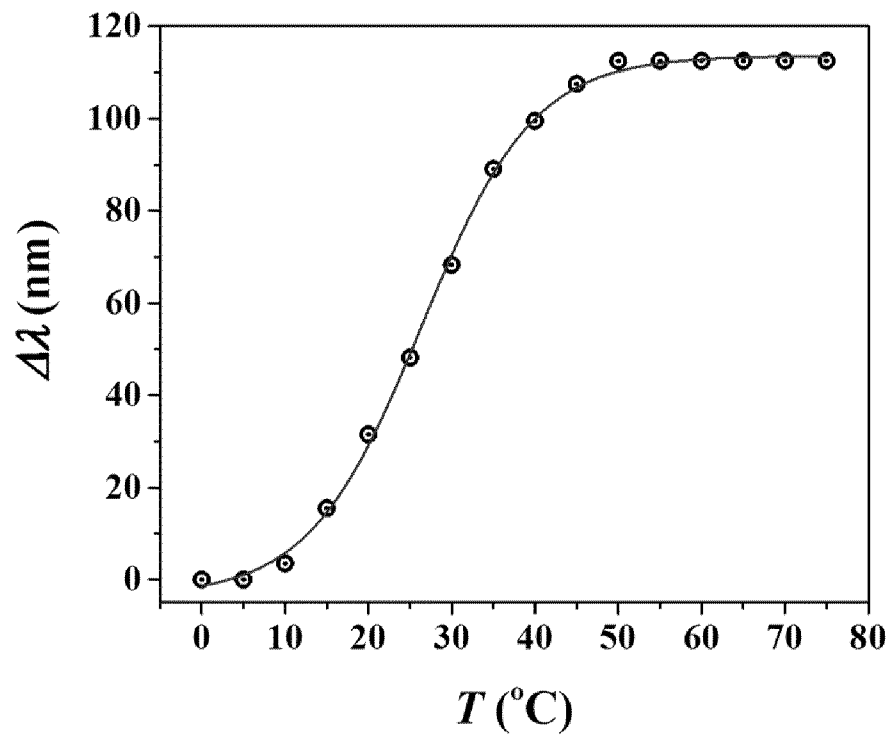


Fig. 17

18/24

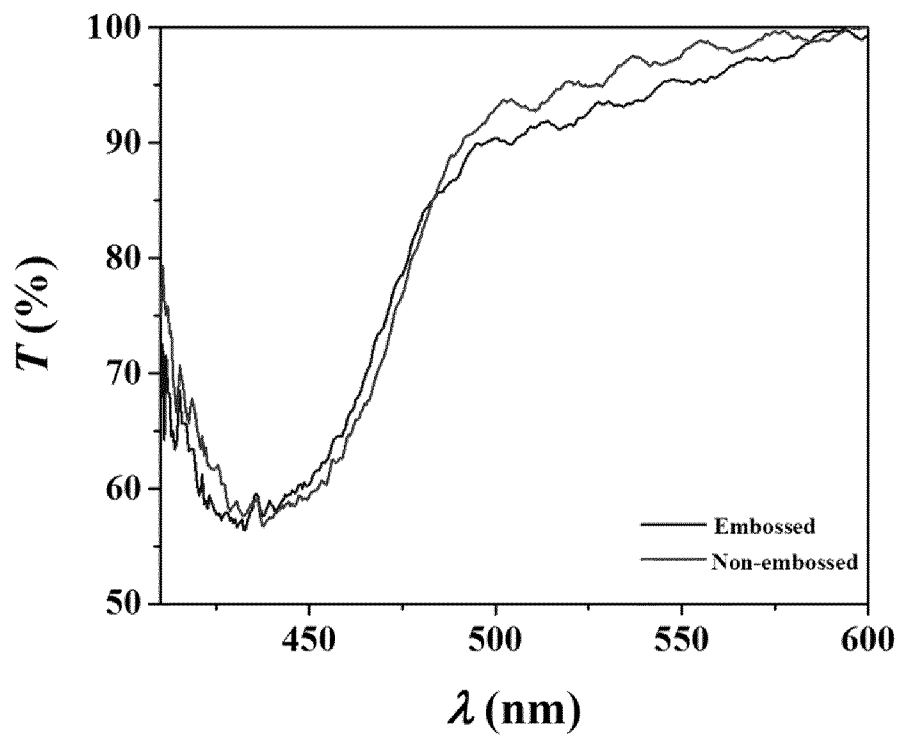


Fig. 18

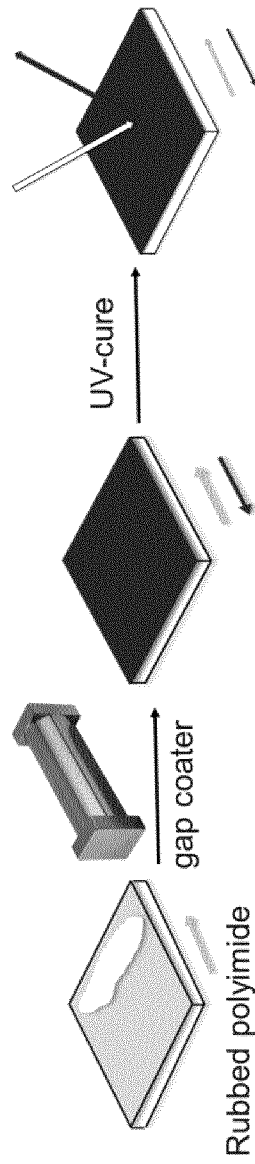


Fig. 19

20/24

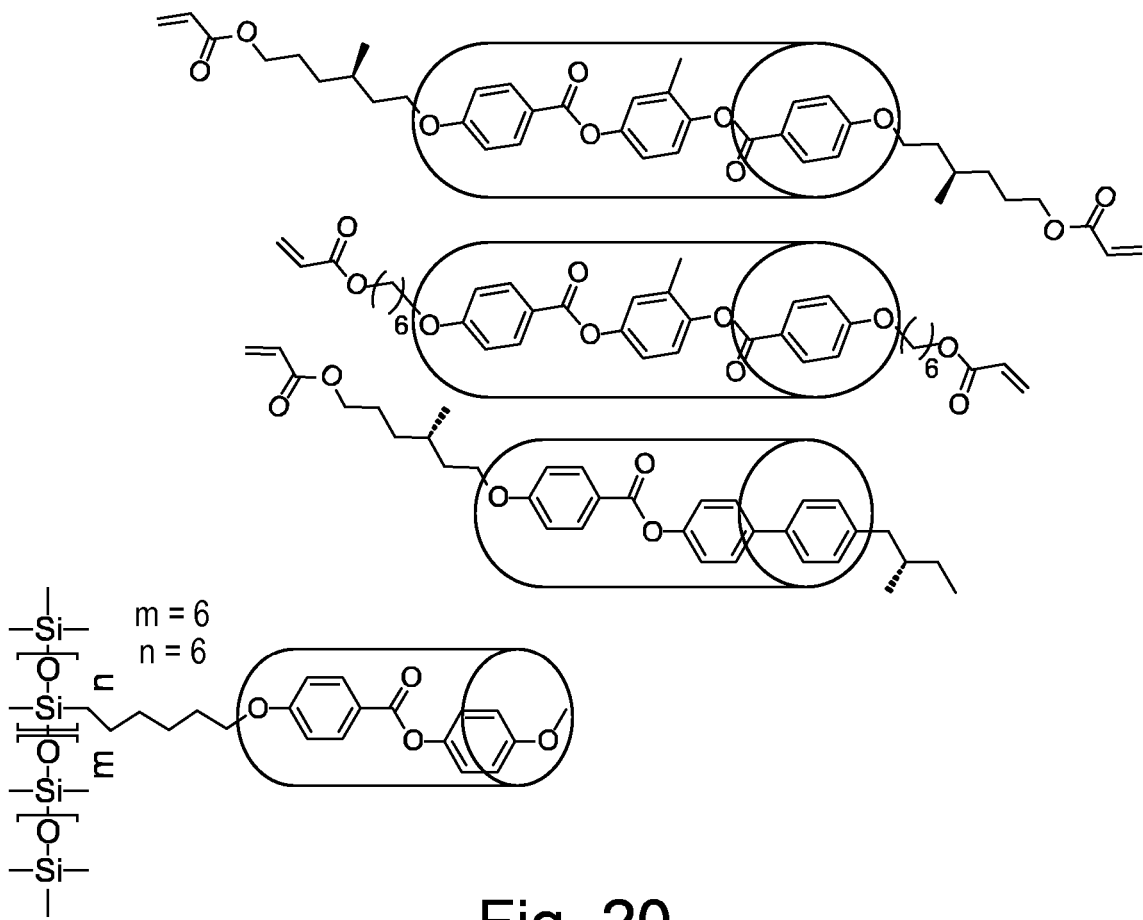
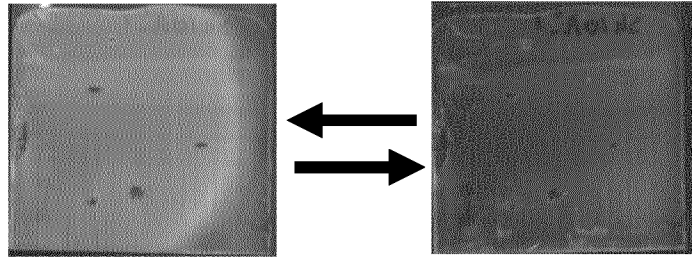


Fig. 20

21/24

A



B

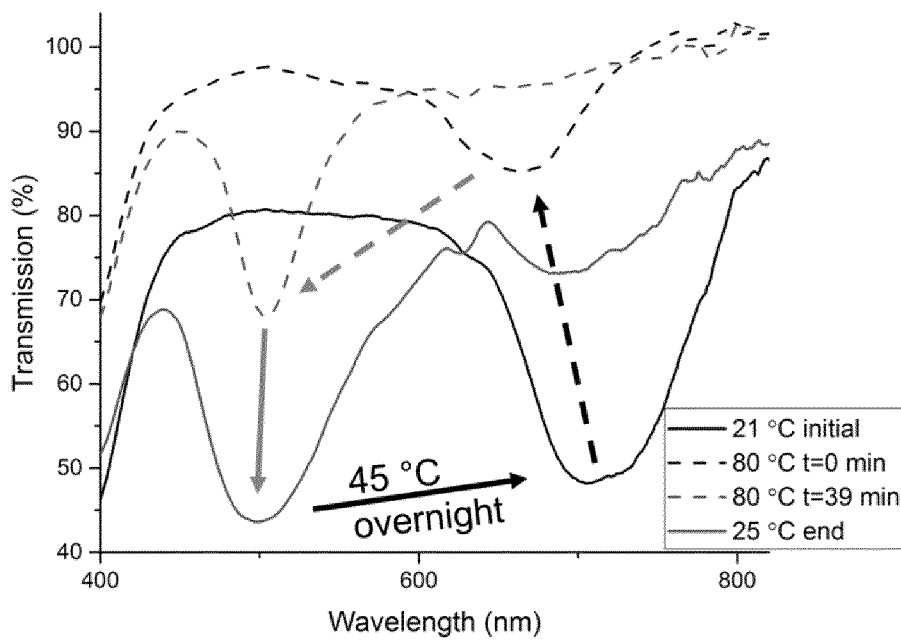


Fig. 21

22/24

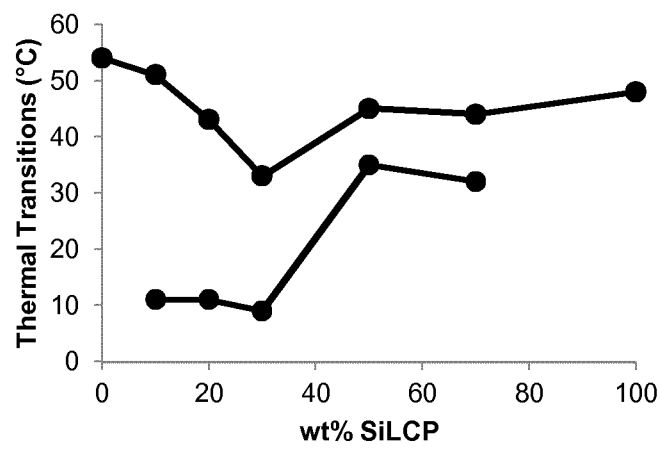


Fig. 22

23/24

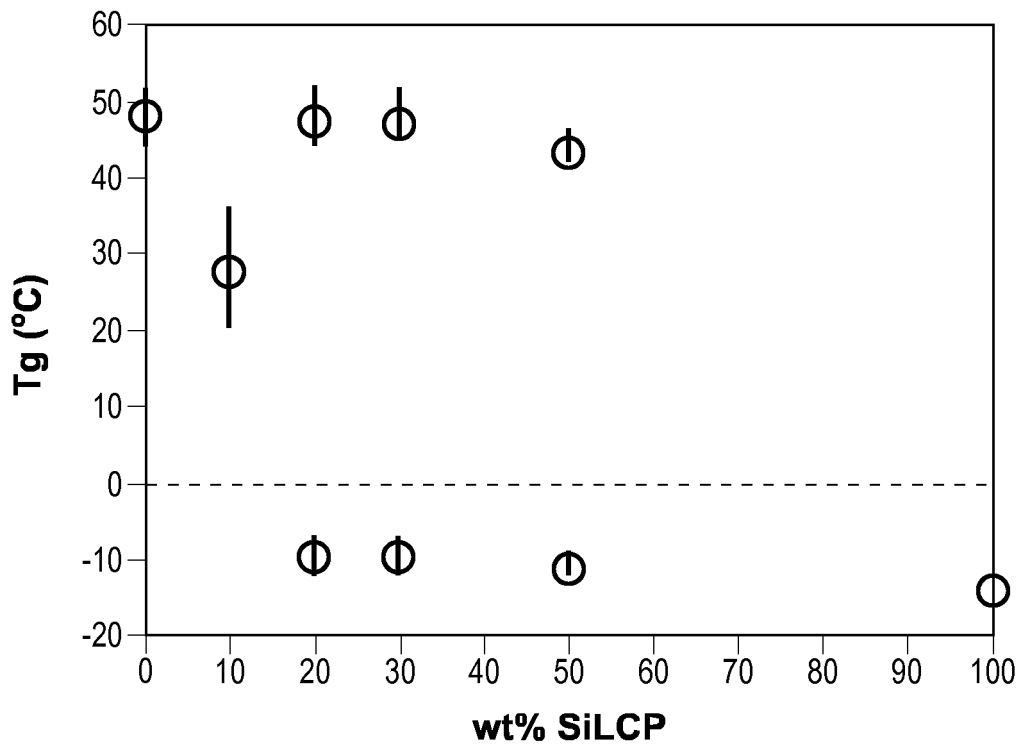


Fig. 23

24/24

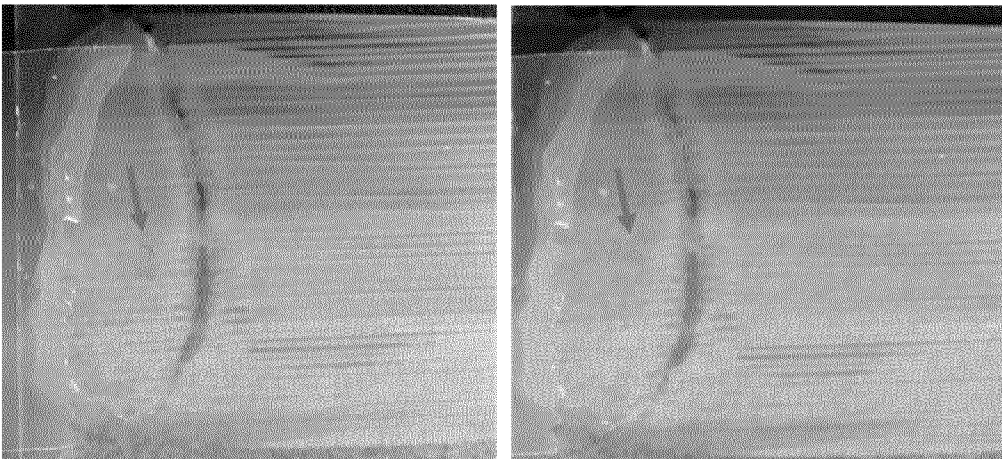


Fig. 24

INTERNATIONAL SEARCH REPORT

International application No
PCT/EP2017/070837

A. CLASSIFICATION OF SUBJECT MATTER
INV. G01K3/04 C09K19/38 C09K19/40 C09K19/04
ADD.
According to International Patent Classification (IPC) or to both national classification and IPC

B. FIELDS SEARCHED
Minimum documentation searched (classification system followed by classification symbols)
G01K C09K

Documentation searched other than minimum documentation to the extent that such documents are included in the fields searched

Electronic data base consulted during the international search (name of data base and, where practicable, search terms used)
EPO-Internal, WPI Data

C. DOCUMENTS CONSIDERED TO BE RELEVANT

| Category* | Citation of document, with indication, where appropriate, of the relevant passages | Relevant to claim No. |
|-----------|--|-----------------------|
| A | US 2016/076947 A1 (RIBI HANS O [US]) 17 March 2016 (2016-03-17) paragraph [0119] paragraph [0053] | 1-12 |
| A | US 5 130 828 A (FERGASON JAMES L [US]) 14 July 1992 (1992-07-14) column 2, line 64 - column 6, line 59 | 1-12 |
| A | WO 85/05467 A (FERGASON J L) 5 December 1985 (1985-12-05) page 3 - page 10 | 1-12 |
| | ----- -/-- | |

Further documents are listed in the continuation of Box C.

See patent family annex.

* Special categories of cited documents :

- "A" document defining the general state of the art which is not considered to be of particular relevance
- "E" earlier application or patent but published on or after the international filing date
- "L" document which may throw doubts on priority claim(s) or which is cited to establish the publication date of another citation or other special reason (as specified)
- "O" document referring to an oral disclosure, use, exhibition or other means
- "P" document published prior to the international filing date but later than the priority date claimed

- "T" later document published after the international filing date or priority date and not in conflict with the application but cited to understand the principle or theory underlying the invention
- "X" document of particular relevance; the claimed invention cannot be considered novel or cannot be considered to involve an inventive step when the document is taken alone
- "Y" document of particular relevance; the claimed invention cannot be considered to involve an inventive step when the document is combined with one or more other such documents, such combination being obvious to a person skilled in the art
- "&" document member of the same patent family

| | |
|--|--|
| Date of the actual completion of the international search 25 October 2017 | Date of mailing of the international search report 07/11/2017 |
| Name and mailing address of the ISA/ European Patent Office, P.B. 5818 Patentlaan 2 NL - 2280 HV Rijswijk Tel. (+31-70) 340-2040, Fax: (+31-70) 340-3016 | Authorized officer Poole, Robert |

INTERNATIONAL SEARCH REPORT

International application No
PCT/EP2017/070837

| C(Continuation). DOCUMENTS CONSIDERED TO BE RELEVANT | | |
|--|--|-----------------------|
| Category* | Citation of document, with indication, where appropriate, of the relevant passages | Relevant to claim No. |
| A | <p>DYLAN J D DAVIES ET AL: "A Printable Optical Time-Temperature Integrator Based on Shape Memory in a Chiral Nematic Polymer Network", ADVANCED FUNCTIONAL MATERIALS, WILEY - V C H VERLAG GMBH & CO. KGAA, DE, vol. 23, no. 21, 6 June 2013 (2013-06-06), pages 2723-2727, XP001582968, ISSN: 1616-301X, DOI: 10.1002/ADFM.201202774 [retrieved on 2013-01-15] figure 4</p> <p style="text-align: center;">-----</p> | 1-12 |

INTERNATIONAL SEARCH REPORT

Information on patent family members

International application No

PCT/EP2017/070837

| Patent document cited in search report | Publication date | Patent family member(s) | Publication date |
|--|------------------|-------------------------|------------------|
| US 2016076947 | A1 | 17-03-2016 | |
| | | US 2010012018 A1 | 21-01-2010 |
| | | US 2012266806 A1 | 25-10-2012 |
| | | US 2014145112 A1 | 29-05-2014 |
| | | US 2016076947 A1 | 17-03-2016 |
| | | WO 2010009441 A2 | 21-01-2010 |
| ----- | | | |
| US 5130828 | A | 14-07-1992 | NONE |
| ----- | | | |
| WO 8505467 | A | 05-12-1985 | ----- |